JOURNAL OF AIRCRAFT
Vol. 45, No. 2, March–April 2008

Continuation of Higher-Order Harmonic Balance Solutions for Nonlinear Aeroelastic Systems

G. Dimitriadis*
University of Liège, 4000 Liège, Belgium

DOI: 10.2514/1.30472

The harmonic balance method is a very useful tool for characterizing and predicting the response of nonlinear dynamic systems undergoing periodic oscillations, either self-excited or due to harmonic excitation. The method and several of its variants were applied to nonlinear aeroelastic systems over the last two decades. This paper presents a detailed description of several harmonic balance methods and a continuation framework allowing the methods to follow the response of dynamic systems from the bifurcation point to any desired parameter value, while successfully negotiating further fold bifurcations. The continuation framework is described for systems undergoing subcritical and supercritical Hopf bifurcations as well as a particular type of explosive bifurcation. The methods investigated in this work are applied to a nonlinear aeroelastic model of a generic transport aircraft featuring polynomial or free-play stiffness nonlinearity in the control surface. It is shown that high-order harmonic balance solutions will accurately capture the complete bifurcation behavior of this system for both types of nonlinearity. Low-order solutions can become inaccurate in the presence of numerous folds in the limit-cycle oscillation branch but can still yield practical engineering information at a fraction of the cost of higher-order solutions. Time-domain harmonic balance schemes are shown to be more computationally expensive than the standard harmonic balance approach.

I. Introduction

THE study of nonlinear aeroelastic systems has become an increasingly important field of research over the last two decades. It is now recognized by both academics and industry that aircraft can be nonlinear and that the nonlinearity can cause dynamic phenomena such as limit-cycle oscillations (LCOs) that cannot be predicted using linear methods. Additionally, the forced response of nonlinear aeroelastic systems to harmonic excitation depends not only on the frequency of the excitation but also on its amplitude.

One method that has been used for a number of years to characterize and predict nonlinear phenomena is the harmonic balance method. Though some attribute the method to Poincaré, the reference usually quoted as the first complete presentation of harmonic balance is by Kryloff and Bogoliuboff [1]. Since then a number of authors have applied the method to various nonlinear dynamic and aeroelastic systems. Additionally, numerous variants of the method have been proposed, usually in its higher-order form: higher-order harmonic balance (HOHB). The object of all HB methods is to express the periodic response of nonlinear systems (either due to limit-cycle oscillations or harmonic excitation) as the Fourier series that best approximates the true system response.

The harmonic balance method is very efficient when applied to parameter-independent systems but can become computationally expensive when the evolution of system response with varying values of the controlling parameters must be investigated. Several authors have proposed methods for continuing efficiently harmonic balance solutions over a range of parameter values but these approaches are, in general, only applicable to single HB variants. Additionally, little work has been devoted to the rigorous explanation of how the HB continuation can be started at the bifurcation point for various types of bifurcation.

The purpose of this work is threefold. First, to present the harmonic balance method and most of its variants under a unified framework and to demonstrate that many of the variants are conceptually different but practically identical. Second, to facilitate the application of HB methods to parameter-dependent systems undergoing LCOs using a rigorous continuation framework, capable of starting HB solutions at the bifurcation point for three particular types of bifurcation. Finally, to demonstrate the continuation of HB approaches on a nonlinear aeroelastic system of a generic transport aircraft (GTA) with nonlinear stiffness in the aileron deflection angle.

Received 15 February 2007; revision received 6 July 2007; accepted for publication 2 September 2007.

*Assistant Professor, Aerospace and Mechanical Engineering Department, 1 Chemin des Chevreuils; gdimitriadis@ulg.ac.be. Member AIAA.

II. Higher-Order Harmonic Balance

The concept behind the harmonic balance (and its higher orders), as applied to free or forced vibration problems, is very simple. The method attempts to find a Fourier series approximation of the true response of a given nonlinear system that is undergoing limit-cycle oscillations. In other words, it is assumed that the solution of the nonlinear system can be represented as a sum of sine and cosine terms. Consider a general unforced nonlinear system of the form

$$\dot{\mathbf{x}} = \mathbf{f}(\mathbf{x}, t, \mathbf{w}) \tag{1}$$

where $\mathbf{x}(t)$ is a $m \times 1$ vector of system states, t is the time, $\mathbf{w}$ is a $p \times 1$ vector of system parameters, and $\mathbf{f}(\mathbf{x}, t, \mathbf{w})$ is a $m \times 1$ vector of nonlinear functions. The object of harmonic balancing is to approximate periodic solutions of this system, $x(t)$, as a sum of sinusoids. There are two mechanisms by which periodic oscillations can occur: either the system is excited by an external periodic force or it is undergoing self-excited oscillations (LCOs). This paper deals with the latter case, hence the forced response case will not be discussed in length.

Assuming that the system is undergoing LCOs and following the harmonic balance methodology, the states are approximated by

$$\mathbf{x} = \mathbf{X}_0 + \sum_{k=1}^{N} (\mathbf{X}_{k1} \sin k\omega t + \mathbf{X}_{k2} \cos k\omega t) \tag{2}$$

where ω is the fundamental response frequency; $\mathbf{X}_0$, $\mathbf{X}_{k1}$, $\mathbf{X}_{k2}$ are unknown coefficients; and N is the order of the approximation. If the order is chosen as $N = 1$, then the classical first-order HB approximation is obtained. HOHB schemes refer to $N > 1$. To simplify the terminology, the term harmonic balance will be used to denote harmonic balance methods of all orders. Equation (2) is substituted into Eq. (1), yielding

$$\sum_{k=1}^{N}(k\omega\mathbf{X}_{k1}\cos k\omega t - k\omega\mathbf{X}_{k2}\sin k\omega t) = \mathbf{f}\left(\mathbf{X}_0 + \sum_{k=1}^{N}(\mathbf{X}_{k1}\sin k\omega t + \mathbf{X}_{k2}\cos k\omega t)\right) \quad (3)$$

The right-hand side of this expression can be expanded into a sum of sinusoids either using algebraic methods or using Fourier analysis. The result is an equation of motion of the form

$$\sum_{k=1}^{N}(k\omega\mathbf{X}_{k1}\cos k\omega t - k\omega\mathbf{X}_{k2}\sin k\omega t) = \mathbf{F}_0 + \sum_{k=1}^{N}(\mathbf{F}_{k1}\sin k\omega t + \mathbf{F}_{k2}\cos k\omega t) \quad (4)$$

where $\mathbf{F}_0$, $\mathbf{F}_{k1}$, and $\mathbf{F}_{k2}$ are known functions of $\mathbf{w}$, $\mathbf{X}_0$, $\mathbf{X}_{k1}$, $\mathbf{X}_{k2}$, and ω. This equation must be solved for $\mathbf{X}_0$, $\mathbf{X}_{k1}$, $\mathbf{X}_{k2}$, and ω. There are two main approaches to the solution of such equations in the aerospace literature: harmonic balancing and Galerkin's method.

A. Harmonic Balancing

This consists simply of equating the coefficients of every sine and cosine term to zero. In other words, the total coefficients of $\sin\omega t$, $\cos\omega t$, $\sin 2\omega t$, $\cos 2\omega t$, etc., as well as the constant term must be equal to zero for the equations of motion to be satisfied. Harmonic balancing leads to $m(2N+1)$ nonlinear algebraic equations in terms of ω, $\mathbf{X}_0$, $\mathbf{X}_{k1}$, and $\mathbf{X}_{k2}$ of the form

$$\mathbf{F}_0 = \mathbf{0} \qquad k\omega\mathbf{X}_{k2} + \mathbf{F}_{k1} = \mathbf{0} \qquad -k\omega\mathbf{X}_{k1} + \mathbf{F}_{k2} = \mathbf{0} \quad (5)$$

for $k = 1, \ldots, N$ or, in simpler notation,

$$\mathbf{g}(\mathbf{X}_0, \mathbf{X}_{k1}, \mathbf{X}_{k2}, \omega, \mathbf{w}) = \mathbf{0} \quad (6)$$

where $\mathbf{g}$ are nonlinear functions. The solution of these equations yields an approximation of the true LCO behavior of the nonlinear system for the chosen parameter values. Notice that there are $m \times (2N+1) + 1$ unknowns including the frequency and only $m \times (2N+1)$ equations. This problem can be overcome without loss of generality if, for example, the first element of $\mathbf{X}_{12}$ is set to zero, thus decreasing the number of unknowns to $m \times (2N+1)$. This process is sometimes called *phase fixing*.

B. Galerkin's Procedure

It should be mentioned that the harmonic balance approach is sometimes called the Galerkin [2] or Galerkin–Newton–Raphson [3] method. Lau and Zhang [4] stated that Galerkin methods are exactly equivalent to harmonic balancing. Galerkin's method seeks to solve differential equations using a set of basis functions. For an equation of the type $\dot{\mathbf{x}} = \mathbf{f}(\mathbf{x}, t, \mathbf{w})$, a solution is sought of the form

$$\mathbf{x} = \mathbf{c}_0\phi_0(t) + \sum_{k=1}^{N}\mathbf{c}_k\phi_k(t) \quad (7)$$

where $\phi_k(t)$ are basis functions that are orthogonal over a certain interval (say, $[a, b]$). Expressions (7) are substituted into the equations of motion (1), which are then premultiplied by each of the basis functions and integrated over the orthogonality interval, yielding

$$\int_a^b \phi_j(t)\left\{\left(\mathbf{c}_0\dot{\phi}_0(t) + \sum_{k=1}^{N}\mathbf{c}_k\dot{\phi}_k(t)\right) - \mathbf{f}\left(\mathbf{c}_0\phi_0(t) + \sum_{k=1}^{N}\mathbf{c}_k\phi_k(t)\right)\right\}\mathrm{d}t = 0 \quad (8)$$

for $j = 1, \ldots, N$. If the chosen basis functions $\phi_k(t)$ are sinusoidal, so that expression (7) is of the form of Eq. (2), and if the limits of integration are chosen over a full period, then Eq. (8) becomes

$$\int_0^{2\pi/\omega}\left\{\sum_{k=1}^{N}(\mathbf{X}_{k1}k\omega\cos k\omega t - \mathbf{X}_{k2}k\omega\sin k\omega t) - \mathbf{f}\left(\mathbf{X}_0 + \sum_{k=1}^{N}(\mathbf{X}_{k1}\sin k\omega t + \mathbf{X}_{k2}\cos k\omega t)\right)\right\}\mathrm{d}t = \mathbf{0} \quad (9)$$

$$\int_0^{2\pi/\omega}\sin j\omega t\left\{\sum_{k=1}^{N}(\mathbf{X}_{k1}k\omega\cos k\omega t - \mathbf{X}_{k2}k\omega\sin k\omega t) - \mathbf{f}\left(\mathbf{X}_0 + \sum_{k=1}^{N}(\mathbf{X}_{k1}\sin k\omega t + \mathbf{X}_{k2}\cos k\omega t)\right)\right\}\mathrm{d}t = \mathbf{0} \quad (10)$$

$$\int_0^{2\pi/\omega}\cos j\omega t\left\{\sum_{k=1}^{N}(\mathbf{X}_{k1}k\omega\cos k\omega t - \mathbf{X}_{k2}k\omega\sin k\omega t) - \mathbf{f}\left(\mathbf{X}_0 + \sum_{k=1}^{N}(\mathbf{X}_{k1}\sin k\omega t + \mathbf{X}_{k2}\cos k\omega t)\right)\right\}\mathrm{d}t = \mathbf{0} \quad (11)$$

for $j = 1, \ldots, N$. Because of the orthogonality of sinusoidal functions, integrals of the type

$$\int_0^{2\pi/\omega}\cos 2\omega t\cos 3\omega t\,\mathrm{d}t$$

and

$$\int_0^{2\pi/\omega}\sin k\omega t\cos k\omega t\,\mathrm{d}t$$

will vanish, and

$$\int_0^{2\pi/\omega}\sin^2 k\omega t\,\mathrm{d}t = \pi/\omega$$

and

$$\int_0^{2\pi/\omega}\cos^2 k\omega t\,\mathrm{d}t = \pi/\omega$$

The final result is that the Galerkin procedure yields the same $2N+1$ equations as harmonic balancing; that is,

$$\mathbf{g}(\mathbf{X}_0, \mathbf{X}_{k1}, \mathbf{X}_{k2}, \omega, \mathbf{w}) = \mathbf{0} \quad (12)$$

C. Expanding the Nonlinear Function

When substituting expression (2) back into the equation of motion, the nonlinear term becomes a function of the sinusoidal series in this expression. With some nonlinear functions (especially polynomials), it is possible to expand them and reduce the higher-order powers of the sinusoidal terms to higher-order frequencies, so that

$$\mathbf{f}\left(\mathbf{X}_0 + \sum_{k=1}^{N}(\mathbf{X}_{k1}\sin k\omega t + \mathbf{X}_{k2}\cos k\omega t)\right) = \mathbf{F}_0 + \sum_{k=1}^{L}(\mathbf{F}_{k1}\sin k\omega t + \mathbf{F}_{k2}\cos k\omega t) \quad (13)$$

where the order of the right-hand-side summation is denoted by L to demonstrate the fact that nonlinearity will introduce terms of orders that do not exist in the chosen sinusoidal expansion for $\mathbf{x}(t)$. For example, $\cos^2 N\omega t$ will introduce a $\cos 2N\omega t$ term. Some harmonic balance methods truncate the right-hand side of Eq. (13) to order N, as shown in Eq. (4), whereas others use different orders for the *input* and *output* sinusoidal expansions. When $L > N$, the harmonic balance equations (5) are supplemented by additional equations of the form

$$\mathbf{F}_{k1} = \mathbf{0} \qquad \mathbf{F}_{k2} = \mathbf{0}$$

for $k = N+1, \ldots, L$. These additional equations create an overdetermined system with $m(2L+1)$ equations and $m(2N+1)$ unknowns.

Most nonlinear functions do not allow this type of analytical expansion, either because they are too complex or because they are discontinuous or nonanalytic. Such functions are usually expressed directly as Fourier series, so that the $\mathbf{F}_0$, $\mathbf{F}_{k1}$, and $\mathbf{F}_{k2}$ coefficients in Eq. (13) can be obtained from the well-known expressions for the Fourier coefficients; that is,

$$\begin{aligned}
\mathbf{F}_0 &= \frac{\omega}{2\pi}\int_0^{2\pi/\omega} \mathbf{f}\left(\mathbf{X}_0 + \sum_{k=1}^{N}(\mathbf{X}_{k1}\sin k\omega t + \mathbf{X}_{k2}\cos k\omega t)\right) \mathrm{d}t \\
\mathbf{F}_{k1} &= \frac{\omega}{\pi}\int_0^{2\pi/\omega} \mathbf{f}\left(\mathbf{X}_0 + \sum_{k=1}^{N}(\mathbf{X}_{k1}\sin k\omega t + \mathbf{X}_{k2}\cos k\omega t)\right) \sin k\omega t\, \mathrm{d}t \\
\mathbf{F}_{k2} &= \frac{\omega}{\pi}\int_0^{2\pi/\omega} \mathbf{f}\left(\mathbf{X}_0 + \sum_{k=1}^{N}(\mathbf{X}_{k1}\sin k\omega t + \mathbf{X}_{k2}\cos k\omega t)\right) \cos k\omega t\, \mathrm{d}t
\end{aligned} \tag{14}$$

Identical integrals are obtained from the Galerkin procedure equations (9–11). This approach is taken, for example, by Pierre et al. [5] and Lau and Zhang [4]. Strictly speaking, the preceding Fourier expressions require that the functions $\mathbf{f}$ be analytic, continuous, and integrable between the limits of integration. However, if the integrations are carried out numerically, then these requirements are relaxed. If the functions can be evaluated numerically at $2N+1$ time instances $t_r = 0, 2\pi/\omega(2N+1), \ldots, 4\pi N/\omega(2N+1)$, then the Fourier coefficients can be approximated using summations; that is,

$$\begin{aligned}
\mathbf{F}_0 &= \frac{1}{2N+1}\sum_{r=0}^{2N}\mathbf{f}(\mathbf{x}_r) \qquad \mathbf{F}_{k1} = \frac{2}{2N+1}\sum_{r=0}^{2N}\mathbf{f}(\mathbf{x}_r)\sin k\omega t_r \\
\mathbf{F}_{k2} &= \frac{2}{2N+1}\sum_{r=0}^{2N}\mathbf{f}(\mathbf{x}_r)\cos k\omega t_r
\end{aligned} \tag{15}$$

Liu et al. [6,7] expressed these summations as a matrix product of the form

$$\begin{Bmatrix} \mathbf{F}_0 \\ \mathbf{F}_{k1} \\ \mathbf{F}_{k2} \end{Bmatrix} = \frac{2}{2N+1}\begin{pmatrix} \frac{1}{2}\mathbf{I} & \frac{1}{2}\mathbf{I} & \cdots & \frac{1}{2}\mathbf{I} \\ \sin k\omega t_0\mathbf{I} & \sin k\omega t_1\mathbf{I} & \cdots & \sin k\omega t_{2N}\mathbf{I} \\ \cos k\omega t_0\mathbf{I} & \cos k\omega t_1\mathbf{I} & \cdots & \cos k\omega t_{2N}\mathbf{I} \end{pmatrix}\begin{Bmatrix} \mathbf{f}(\mathbf{x}_0) \\ \vdots \\ \mathbf{f}(\mathbf{x}_{2N}) \end{Bmatrix} \tag{16}$$

for $k = 1, \ldots, N$, where $\mathbf{I}$ is a $m \times m$ unit matrix. It should be noted that the matrix in this equation contains many zeros so that a straight matrix multiplication becomes inefficient.

Of course, this treatment can also be applied to nonlinear functions that allow analytical expansions, thus avoiding the need to perform complex and system-specific analytical operations. Once the Fourier coefficients have been evaluated, they can be substituted into Eqs. (5) to set up Eqs. (6).

It should be noted that the Fourier coefficients do not have to be evaluated numerically over $2N+1$ time instances. The time-domain signals $\mathbf{x}_r$ can have any desired resolution, so that the number of time instances can be $M \geq 2N+1$.

D. Discrete Fourier Transform Evaluation of Nonlinear Function Fourier Coefficients

Ling and Wu [2] argued that the calculation of the Fourier coefficients of the nonlinear function from the integrals of Eq. (14) or the summations of Eq. (15) is computationally demanding. Instead, they advocated the use of the fast Fourier transform (FFT) to calculate these coefficients. They suggest that the number of points at which $\mathbf{f}(\mathbf{x})$ is realized must be larger than $2N+1$ and equal to a power of 2. Under these circumstances, they demonstrate that the FFT calculation of the Fourier coefficients of $\mathbf{f}(\mathbf{x})$ requires significantly fewer operations. Cameron and Griffin [8] and Leung and Ge [9,10] also chose the FFT to calculate the Fourier coefficients of the nonlinear function.

Kim and Noah [11] obtained the Fourier coefficients from the discrete Fourier transform (DFT) as

$$\begin{aligned}
\mathbf{F}_0 &= \frac{1}{M}\sum_{r=0}^{M-1}\mathbf{f}(\mathbf{x}_r) \qquad \mathbf{F}_{k1} = -\frac{2}{M}\Im\left\{\sum_{r=0}^{M-1}\mathbf{f}(\mathbf{x}_r)e^{J(-\frac{2\pi kr}{M})}\right\} \\
\mathbf{F}_{k2} &= \frac{2}{M}\Re\left\{\sum_{r=0}^{M-1}\mathbf{f}(\mathbf{x}_r)e^{J(-\frac{2\pi kr}{M})}\right\}
\end{aligned} \tag{17}$$

where $J = \sqrt{-1}$, $\Im$ denotes the imaginary part of a complex number, and $\Re$ denotes the real part.

E. Harmonic Balance with Newton–Raphson

Because the crux of the higher-order harmonic balance method is the solution of a system of nonlinear algebraic equations, it was not seriously considered as a possibility before the late 1970s, when computers capable of such calculations started appearing. One of the first successful implementations of a HOHB approach is the multiharmonic balance technique of Tamura et al. [12] in 1981. They presented a complete HOHB methodology, much of which is still being used today by many authors. They handled the nonlinear term by expressing it as a Fourier series, and they solved the nonlinear algebraic problem of Eq. (6) using a Newton–Raphson procedure. Many subsequent publications by other researchers describe exactly the same procedure.

Define $\mathbf{a} = [\,\mathbf{X}_0 \quad \mathbf{X}_{k1} \quad \mathbf{X}_{k2} \quad \omega\,]^T$ to be a vector containing all the unknowns of Eq. (6). Then the equation can be written as

$$\mathbf{g}(\mathbf{a}) = \mathbf{0} \tag{18}$$

Assume that an ith estimate of the solution vector $\mathbf{a}_i$ is available and that its associated residual is $\mathbf{g}(\mathbf{a}_i)$. A better estimate, $\mathbf{a}_i + \Delta\mathbf{a}_i$, is required, which has a residual of zero. Substituting this estimate into Eq. (18) and expanding in a first-order Taylor series leads to

$$\mathbf{g}(\mathbf{a}_i + \Delta\mathbf{a}_i) = \mathbf{g}(\mathbf{a}_i) + \left.\frac{\partial \mathbf{g}}{\partial \mathbf{a}}\right|_{\mathbf{a}_i}\Delta\mathbf{a}_i = \mathbf{0} \tag{19}$$

By the Newton–Raphson method, if an ith estimate for $\mathbf{a}$ is available (say, $\mathbf{a}_i$), then a better estimate can be calculated as

$$\mathbf{a}_{i+1} = \mathbf{a}_i + \Delta\mathbf{a}_i \tag{20}$$

where $\Delta\mathbf{a}_i$ can be obtained from the solution of

$$\left.\frac{\partial \mathbf{g}}{\partial \mathbf{a}}\right|_{\mathbf{a}_i}\Delta\mathbf{a}_i = -g(\mathbf{a}_i) \tag{21}$$

In other words, the improvement to the ith estimate is equal to the inverse of the Jacobian matrix evaluated around the ith estimate times the value of the nonlinear functions at $\mathbf{a}_i$. After a number of iterations, the values of the estimated $\mathbf{a}_i$ coefficients will converge. They can then be substituted into Eq. (2) to yield a complete sinusoidal approximation to the true response of the nonlinear system.

The main difficulty of the Newton–Raphson method is the calculation of the Jacobian. In some cases, the functions $\mathbf{g}(\mathbf{a})$ are analytic and simple enough to allow the derivation of analytical forms for the elements of the Jacobian matrix. However, it is quite possible that $\mathbf{g}(\mathbf{a})$ will not allow analytical forms for the Jacobian. In this case, the latter is estimated numerically; that is,

$$\left.\frac{\partial \mathbf{g}}{\partial \mathbf{a}}\right|_{\mathbf{a}_i} = \frac{\mathbf{g}(\mathbf{a}_i + \delta a) - \mathbf{g}(\mathbf{a}_i)}{\delta a} \tag{22}$$

where δa is a small increment to each of the elements of $\mathbf{a}$. Equation (22) is deceptively simple because it disguises the true amount of required computation. For each of the elements of the Jacobian matrix, the corresponding element of $\mathbf{a}$ is increased by δa, whereas all the other elements are kept constant. Thus, if $\mathbf{a}$ has n elements, then $\mathbf{g}$ must be computed $n + 1$ times for a total of $n \times (n + 1)$ calculations (or $n \times n$ calculations if one of the amplitudes was set to zero).

F. Newton–Raphson Versus Broyden

Ling and Wu [2] introduced a further innovation in the harmonic balance methodology: the solution of the simultaneous nonlinear equations by Broyden's method [13] rather than Newton–Raphson. Here, the two methods will be discussed and their relative merits pointed out.

As mentioned previously, a disadvantage of the Newton–Raphson method is that the Jacobian must be calculated explicitly at each iteration. An additional disadvantage is the fact that the procedure can fail to converge. The initial guess $\mathbf{a}_0$ must be reasonably close to the true solution to ensure convergence. On the other hand, when the scheme converges, it converges quite quickly. A simple way to improve the chances of convergence is to delay the convergence rate; that is, replace Eq. (20) by

$$\mathbf{a}_{i+1} = \mathbf{a}_i + \Omega \Delta \mathbf{a}_i \tag{23}$$

where Ω is the relaxation factor, a suitable positive real number less than 1. The lower the value of Ω, the slower the convergence rate. However, the improvement in the probability of convergence can be marginal.

Broyden [13] developed a class of quasi-Newton methods for the solution of nonlinear algebraic equations that do not require the explicit calculation of the Jacobian at each time step. Equation (20) is replaced by

$$\mathbf{a}_{i+1} = \mathbf{a}_i - \mathbf{A}_i^{-1}\mathbf{g}(\mathbf{a}_i) \tag{24}$$

where $\mathbf{A}_i$ is an approximation to the Jacobian matrix. Broyden [13] showed that $\mathbf{A}_{i+1}$ can be obtained from the earlier approximation $\mathbf{A}_i$ using

$$\mathbf{A}_{i+1} = \mathbf{A}_i + \frac{(\mathbf{y}_i - \mathbf{A}_i\mathbf{s}_i)\mathbf{s}_i^T}{\mathbf{s}_i \cdot \mathbf{s}_i} \tag{25}$$

where

$$\mathbf{s}_i = \mathbf{a}_{i+1} - \mathbf{a}_i \qquad \mathbf{y}_i = \mathbf{g}(\mathbf{a}_{i+1}) - \mathbf{g}(\mathbf{a}_i)$$

Thus, as soon as the new estimate $\mathbf{a}_{i+1}$ is calculated, the new value of the approximate Jacobian can be obtained directly from Eq. (25), without the need to carry out numerical differentiations of the type shown in Eq. (21). Numerical differentiation is only necessary for the estimation of the initial matrix $\mathbf{A}_0$, which can be taken to be equal to the initial Jacobian matrix. A relaxation factor Ω can be used to facilitate convergence and Broyden [13] gave some guidelines for choosing its value.

It is obvious that Broyden's [13] method requires fewer computations per iteration because of its handling of the Jacobian. Ling and Wu [2] stated that Broyden's [13] method converges more slowly than Newton–Raphson, but the total computation time is shorter because each iteration is less computationally demanding. However, it should be pointed out that there is no guarantee that $\mathbf{A}_{i+1}$ will always be nonsingular.

G. Simplification for Systems with Few Nonlinear States

Higher-harmonic-balance approaches can be very computationally demanding, possibly even more so than the numerical integration (time marching) of the equations of motion. The number of unknowns in a typical HOHB iteration is $m(2N + 1)$, which can be very high for a large system such as an aircraft featuring many harmonics in its response. Accordingly, the Jacobian is a square matrix of size $m(2N + 1) \times m(2N + 1)$. Therefore, practical applications of the methodology must take advantage of all possible simplifications to reduce the number of unknowns.

The application of HOHB techniques to systems with few nonlinear states can be significantly speeded up by treating such systems as a superposition of a small nonlinear system and a large linear system [14]. Here, a nonlinear state is defined as a state on which at least one of the system's nonlinearities depends. Aeroelastic systems with concentrated structural nonlinearities fall into this category. Consider a nonlinear system of the type shown in Eq. (1) but with only one nonlinear state (say, x_n). The equation of motion can be written as

$$\dot{\mathbf{x}} = \mathbf{Q}(\mathbf{w})\mathbf{x} + \mathbf{f}(x_n, \mathbf{w}) \tag{26}$$

where $\mathbf{Q}$ is a $m \times m$ matrix and $\mathbf{f}(x_n, \mathbf{w})$ is a $m \times 1$ vector of nonlinear functions of x_n only. The nonlinear state x_n is expanded as usual

$$x_n = X_0 + \sum_{k=1}^{N}(X_{k1}\sin k\omega t + X_{k2}\cos k\omega t) \tag{27}$$

leading to a nonlinear force of the type

$$\mathbf{f}\left(X_0 + \sum_{k=1}^{N}(X_{k1}\sin k\omega t + X_{k2}\cos k\omega t)\right) = \mathbf{F}_0 + \sum_{k=1}^{N}(\mathbf{F}_{k1}\sin k\omega t + \mathbf{F}_{k2}\cos k\omega t) \tag{28}$$

Once the $\mathbf{F}_0$, $\mathbf{F}_{k1}$, and $\mathbf{F}_{k2}$ coefficients are evaluated (from initial guesses for X_0, X_{k1}, X_{k2}, and ω) the nonlinear force becomes a known function of time $\mathbf{f}(t)$. This function of time effectively acts as the excitation force for an equivalent forced linear system; that is,

$$\dot{\mathbf{x}} = \mathbf{Q}\mathbf{x} + \mathbf{F}_0 + \sum_{k=1}^{N}(\mathbf{F}_{k1}\sin k\omega t + \mathbf{F}_{k2}\cos k\omega t) \tag{29}$$

Because the excitation is harmonic, the response will also be harmonic; in other words,

$$\mathbf{x} = \hat{\mathbf{X}}_0 + \sum_{k=1}^{N}(\hat{\mathbf{X}}_{k1}\sin k\omega t + \hat{\mathbf{X}}_{k2}\cos k\omega t) \tag{30}$$

where $\hat{\mathbf{X}}_0$, $\hat{\mathbf{X}}_{k1}$, and $\hat{\mathbf{X}}_{k2}$ are $m \times 1$ vectors of constants to be evaluated.

Solving the linear forced response problem leads to

$$\mathbf{Q}\,\hat{\mathbf{X}}_0 = -\mathbf{F}_0 \tag{31}$$

and

$$\begin{pmatrix} \mathbf{Q} & k\omega\mathbf{I} \\ -k\omega\mathbf{I} & \mathbf{Q} \end{pmatrix}\begin{Bmatrix} \hat{\mathbf{X}}_{k1} \\ \hat{\mathbf{X}}_{k2} \end{Bmatrix} = \begin{Bmatrix} -\mathbf{F}_{k1} \\ -\mathbf{F}_{k2} \end{Bmatrix} \tag{32}$$

for $k = 1, \ldots, N$, which are systems of linear algebraic equations to be solved for the unknowns $\hat{\mathbf{X}}_0$, $\hat{\mathbf{X}}_{k1}$, and $\hat{\mathbf{X}}_{k2}$. Now there are two estimates for x_n: the original guess of expression (27) and the solution of the forced response problem. For the HOHB solution to be unique, these two estimates must be equal; that is,

$$X_0 + \sum_{k=1}^{N}(X_{k1}\sin k\omega t + X_{k2}\cos k\omega t) = \hat{X}_{0_n} + \sum_{k=1}^{N}(\hat{X}_{k1_n}\sin k\omega t + \hat{X}_{k2_n}\cos k\omega t) \tag{33}$$

where $\hat{X}_{0_n}$, $\hat{X}_{k1_n}$, and $\hat{X}_{k2_n}$ denote the nth elements of vectors $\hat{\mathbf{X}}_0$, $\hat{\mathbf{X}}_{k1}$, and $\hat{\mathbf{X}}_{k2}$. The governing equations of the HOHB scheme become

$$X_0 - \hat{X}_{0_n} = 0 \qquad X_{k1} - \hat{X}_{k1_n} = 0 \qquad X_{k2} - \hat{X}_{k2_n} = 0 \tag{34}$$

for $k = 1, \ldots, N$. Equations (34) are the equivalent of Eqs. (18) for systems with few nonlinear states. In this case, $\mathbf{a} = [X_0 \quad X_{k1} \quad X_{k2} \quad \omega]^T$. In total, these are $2N + 1$ equations with $2N + 1$ unknowns instead of $m(2N + 1)$ equations with $m(2N + 1)$ unknowns. The computational savings of this approach are obvious. In general, the number of unknowns is equal to $l(2N + 1)$, where l is the number of nonlinear states. If all the states are nonlinear, then Eqs. (34) are identical to Eqs. (18).

H. Simplification for Systems with Weak Higher Harmonics

Popov [15] proposed a special harmonic balance scheme for systems with low-amplitude higher harmonics. Instead of the sinusoidal expansion (2), he chose the following series:

$$\mathbf{x} = \mathbf{u}(t) + \varepsilon \mathbf{v}(t) \tag{35}$$

where

$$\mathbf{u}(t) = \mathbf{X}_0 + \mathbf{X}_{11} \sin \omega t + \mathbf{X}_{12} \cos \omega t$$

$$\mathbf{v}(t) = \sum_{k=2}^{N} (\mathbf{X}_{k1} \sin k\omega t + \mathbf{X}_{k2} \cos k\omega t)$$

and ε is a small number. Equation (35) clearly denotes that the dominant term in the system's response is the first-order term, whereas the higher-order terms have small contributions. Substituting back into the equation of motion (1) yields

$$\dot{\mathbf{u}} + \varepsilon \dot{\mathbf{v}} = \mathbf{f}(\mathbf{u} + \varepsilon \mathbf{v}) \tag{36}$$

The nonlinear function can be expanded as a Taylor series around $\mathbf{u}$ to give

$$\dot{\mathbf{u}} + \varepsilon \dot{\mathbf{v}} = \mathbf{f}(\mathbf{u}) + \left.\frac{\partial \mathbf{f}}{\partial \mathbf{u}}\right|_{\mathbf{u}} \varepsilon \mathbf{v} \tag{37}$$

Finally, orders of ε^0 and ε^1 are equated to yield

$$\dot{\mathbf{u}} - \mathbf{f}(\mathbf{u}) = 0 \tag{38}$$

$$\dot{\mathbf{v}} - \left.\frac{\partial \mathbf{f}}{\partial \mathbf{u}}\right|_{\mathbf{u}} \mathbf{v} = 0 \tag{39}$$

The advantage of the Popov [15] approach is that the first-order harmonic balance solution can be sought independently using Eq. (38). Then it is corrected by the addition of the higher harmonics obtained from Eq. (39). There is a wealth of literature on the first-order harmonic balance but it is beyond the scope of this paper.

Lee et al. [16] applied Popov's [15] method to a pitch-plunge airfoil with cubic nonlinear stiffness and obtained responses similar to those from a full third-order harmonic balance scheme for some of the cases they investigated.

I. Incremental Harmonic Balance

The response of many dynamic systems depends on the value of some governing parameters. The harmonic balance method, as described in the previous sections, only yields one converged solution of the equations of motion at one set of parameter values. Lau et al. [17,18] first discussed a method for extending this solution to other parameter values, usually called the incremental harmonic balance (IHB) method. As will be shown later, the method itself results in equations of motion identical to those obtained from the harmonic-balance/Newton–Raphson combination. However, the innovation of the IHB is the consideration of changes in parameter values and the use of a predictor–corrector algorithm.

It is assumed that the full system response $\mathbf{x}_0(t)$ is known at a particular value of the system parameters $\mathbf{w}_0$ and that it is periodic. Then the response for a neighboring set of parameter values

$$\mathbf{w} = \mathbf{w}_0 + \Delta \mathbf{w} \tag{40}$$

can be written as

$$\mathbf{x} = \mathbf{x}_0 + \Delta \mathbf{x} \tag{41}$$

Expressions (40) and (41) are substituted into the equation of motion (1) to yield

$$\dot{\mathbf{x}}_0 + \Delta \dot{\mathbf{x}} = \mathbf{f}(\mathbf{x}_0 + \Delta \mathbf{x}, t, \mathbf{w}_0 + \Delta \mathbf{w}) \tag{42}$$

where $\Delta \dot{\mathbf{x}} = \mathrm{d}(\Delta \mathbf{x})/\,\mathrm{d}t$. Lau et al. [17,18] then expanded Eq. (42) by means of a first-order Taylor expansion, yielding

$$\dot{\mathbf{x}}_0 + \Delta \dot{\mathbf{x}} = \mathbf{f}(\mathbf{x}_0) + \left.\frac{\partial \mathbf{f}}{\partial \mathbf{x}}\right|_{\mathbf{x}_0, \mathbf{w}_0} \Delta \mathbf{x} + \left.\frac{\partial \mathbf{f}}{\partial \mathbf{w}}\right|_{\mathbf{x}_0, \mathbf{w}_0} \Delta \mathbf{w} \tag{43}$$

where $\partial \mathbf{f}/\partial \mathbf{x}|_{\mathbf{x}_0, \mathbf{w}_0}$ is the system's Jacobian matrix at $(\mathbf{x}_0, \mathbf{w}_0)$ and $\partial \mathbf{f}/\partial \mathbf{w}|_{\mathbf{x}_0, \mathbf{w}_0}$ is the parametric gradient matrix. Equation (43) can be rearranged as

$$\Delta \dot{\mathbf{x}} - \left.\frac{\partial \mathbf{f}}{\partial \mathbf{x}}\right|_{\mathbf{x}_0, \mathbf{w}_0} \Delta \mathbf{x} - \left.\frac{\partial \mathbf{f}}{\partial \mathbf{w}}\right|_{\mathbf{x}_0, \mathbf{w}_0} \Delta \mathbf{w} = \mathbf{R}_0 \tag{44}$$

where the residual term $\mathbf{R}_0$ is given by $\mathbf{R}_0 = -\dot{\mathbf{x}}_0 + \mathbf{f}(\mathbf{x}_0, \mathbf{w}_0)$. Equations (44) are a set of linear differential equations in $\Delta \mathbf{x}$ with time-varying coefficients. If $(\mathbf{x}_0, \mathbf{w}_0)$ is an exact solution of the equations of motion, then the residual will be equal to zero. If $(\mathbf{x}_0, \mathbf{w}_0)$ is an initial guess, then corrective terms $(\Delta \mathbf{x}, \Delta \mathbf{w})$ are sought, such that $\mathbf{R}$ is reduced. The ultimate goal is to minimize $\mathbf{R}$.

The known response and the response increment are written as a sinusoidal series; that is,

$$\mathbf{x}_0 = \mathbf{X}_{0,0} + \sum_{k=1}^{N} (\mathbf{X}_{k1,0} \sin k\omega t + \mathbf{X}_{k2,0} \cos k\omega t)$$

$$\Delta \mathbf{x} = \Delta \mathbf{X}_0 + \sum_{k=1}^{N} (\Delta \mathbf{X}_{k1} \sin k\omega t + \Delta \mathbf{X}_{k2} \cos k\omega t) \tag{45}$$

and substituted back into Eq. (44). A Galerkin procedure is then applied and the IHB governing equation is obtained:

$$\mathbf{T}_1 \Delta \mathbf{a} + \mathbf{T}_2 \Delta \mathbf{w} = \mathbf{T}_0 \tag{46}$$

where $\Delta \mathbf{a} = [\Delta \mathbf{X}_0 \quad \Delta \mathbf{X}_{k1} \quad \Delta \mathbf{X}_{k2}]^T$, $\mathbf{T}_0$ is a $m(2N + 1) \times 1$ vector of residuals, $\mathbf{T}_1$ is a $m(2N + 1) \times m(2N + 1)$ matrix, and $\mathbf{T}_2$ is a $m(2N + 1) \times p$ matrix. These equations can be solved for $\Delta \mathbf{w} = \mathbf{0}$ to obtain a better approximation of the true response $\mathbf{x}_1 = \mathbf{x}_0 + \Delta \mathbf{x}$. This $(\mathbf{x}_1, \mathbf{w}_0)$ solution will have an associated residual $\mathbf{R}_1$. Successive reapplication of the IHB procedure can yield approximate system responses with progressively lower residuals. This is known as the *corrector step* of the IHB. In fact, setting $\Delta \mathbf{w} = \mathbf{0}$, Eqs. (46) become

$$\mathbf{T}_1 \Delta \mathbf{a} = \mathbf{T}_0 \tag{47}$$

Notice the similarity between Eq. (47) and the harmonic balance with Newton–Raphson equation (21). In fact, Ferri [19] showed that the sets of equations resulting from the two methods are identical. The only difference between the methods is the order in which the Taylor expansion and the Galerkin procedure are applied. It follows that Eq. (18) can be expanded for a parametric increment $\Delta \mathbf{w}$ as well as a solution increment $\Delta \mathbf{x}$ to yield

$$\left.\frac{\partial \mathbf{g}}{\partial \mathbf{a}}\right|_{\mathbf{a}_0, \mathbf{w}_0} \Delta \mathbf{a} + \left.\frac{\partial \mathbf{g}}{\partial \mathbf{w}}\right|_{\mathbf{a}_0, \mathbf{w}_0} \Delta \mathbf{w} = -g(\mathbf{a}_0) \tag{48}$$

and, by the same argument, Eqs. (48) are identical to Eqs. (46). Incidentally, if Eqs. (48) or Eqs. (46) are applied to a converged

solution at $\mathbf{w}_0$, then an estimate of the solution at $\mathbf{w}_0 + \Delta\mathbf{w}$ will be obtained. This is known as the *predictor step* of the IHB (or harmonic balance with Newton–Raphson) methodology.

The incremental harmonic balance method was proposed for systems excited by a sinusoidal force of known frequency. Therefore, the fundamental response frequency ω is assumed to be known and equal to the excitation frequency. Lau and Yuen [20] extended the IHB methodology to autonomous systems by assuming that the solution $\mathbf{x}_0$ has a fundamental frequency ω_0. Then the nearby solution $\mathbf{x}_0 + \Delta\mathbf{x}$ will have a frequency of $\omega_0 + \Delta\omega$. Equation (44) becomes

$$\Delta\dot{\mathbf{x}} - \left.\frac{\partial\mathbf{f}}{\partial\mathbf{x}}\right|_{\mathbf{x}_0,\mathbf{w}_0,\omega_0}\Delta\mathbf{x} - \left.\frac{\partial\mathbf{f}}{\partial\mathbf{w}}\right|_{\mathbf{x}_0,\mathbf{w}_0,\omega_0}\Delta\mathbf{w} - \left.\frac{\partial\mathbf{f}}{\partial\omega}\right|_{\mathbf{x}_0,\mathbf{w}_0,\omega_0}\Delta\omega = \mathbf{R}_0 \quad (49)$$

where $\mathbf{R}_0 = -\dot{\mathbf{x}}_0 + \mathbf{f}(\mathbf{x}_0, \mathbf{w}_0, \omega_0)$. Relations (45) are substituted into Eqs. (49) and a Galerkin procedure is applied to yield

$$\mathbf{T}_1^- \Delta\mathbf{a} + \mathbf{T}_2\Delta\mathbf{w} + \mathbf{T}_3\Delta\omega = \mathbf{T}_0 \quad (50)$$

where $\mathbf{T}_3$ is a $m(2N+1) \times 1$ vector. As mentioned previously, the introduction of the frequency as an unknown must be offset by setting one of the amplitudes to zero (e.g., the first element of $\Delta\mathbf{X}_{12}$). Therefore, $\mathbf{T}_1^-$ is identical to $\mathbf{T}_1$ except that it is missing a column. If $\Delta\mathbf{a}$ is defined as $\Delta\mathbf{a} = [\,\Delta\mathbf{X}_0 \quad \Delta\mathbf{X}_{k1} \quad \Delta\mathbf{X}_{k2} \quad \omega\,]^T$, then Eqs. (50) can be rewritten as $\mathbf{T}_1^-\Delta\mathbf{a} + \mathbf{T}_2\Delta\mathbf{w} = \mathbf{T}_0$ and they will still be identical to the equivalent equations obtained from the harmonic balance with Newton scheme.

Because of the duality between the two methods, they will be collectively termed *harmonic balance* in this work and no distinction will be made between them. As a historical note, a number of works using the incremental harmonic balance term were published after the initial work by Lau et al. [17,18]. The IHB method was first applied to a two-degree-of-freedom (2-DOF) system by Pierre et al. [5]. Leung and Chui [21] also applied the method to a 2-DOF system: two coupled Duffing oscillators. The IHB term has survived into the 2000s (e.g., Xu et al. [22]). Chung et al. [23] chose the term *perturbation incremental method* to refer to the IHB.

Leung and Ge [9] used the DFT methodologies in conjunction with the incremental harmonic balance. Instead of sinusoidal series of the form of Eqs. (45), a truncated Fourier series with complex coefficients was employed; that is,

$$\mathbf{x}_0 = \sum_{k=-N}^{N} \mathbf{X}_{k,0} e^{jkt} \qquad \Delta\mathbf{x} = \sum_{k=-N}^{N} \Delta\mathbf{X}_k e^{jkt} \quad (51)$$

where $\mathbf{X}_{k,0}$ and $\Delta\mathbf{X}_k$ are complex. After substituting back into Eq. (44), they performed an inverse discrete Fourier transform (IDFT) to obtain the system of linear algebraic equations:

$$\mathbf{J}\,\Delta\mathbf{X} = \mathbf{R} \quad (52)$$

where $\mathbf{J}$ is the Jacobian matrix, $\mathbf{R}$ is the vector of residuals, and $\Delta\mathbf{X}$ is a vector containing all the $\Delta\mathbf{X}_k$. Because the IDFT is essentially a form of numerical integration, its application is equivalent to the Galerkin procedure. Leung and Ge [9] stated that their approach is better than the standard IHB because the resulting Jacobian matrix is, or can be transformed into, a Toeplitz matrix. Systems of simultaneous linear algebraic equations involving Toeplitz matrices require fewer calculations to solve than general systems of equations. The same authors applied the Toeplitz Jacobian matrix approach to systems with discontinuous nonlinearities [10].

Equations (46) or Eqs. (50) can be solved either with $\Delta\mathbf{w} = 0$ to obtain a better solution at the current parameter values $\mathbf{w}_0$ or with $\Delta\mathbf{w} \neq 0$ to obtain the solution at a new value of the parameters (assuming that $\mathbf{x}_0$ is a satisfactory approximation of the system behavior at $\mathbf{w}_0$). Hence, the IHB technique has two utilities [21]:

1) Given an approximate (or guessed) periodic solution, it can correct it so that it moves closer to the true equilibrium condition

2) Given a converged periodic solution, it can predict a new nearby periodic solution

J. Piecewise-Linear Nonlinearities

Piecewise-linear functions are commonly used to model some nonlinearities in engineering systems. Such nonlinearities can arise as a result of inadequate tolerancing, bad maintenance, or necessity. In general, systems with piecewise-linear nonlinearities can be treated using the Tamura et al. [12] approach (i.e., expressed as a Fourier series). For example, Liu and Dowell [7] applied a harmonic balance method to an airfoil with free-play stiffness in the control surface. This has also been the standard treatment for first-order harmonic balance calculations, such as those performed by Yang and Zhao [24]. Nevertheless, several researchers have developed higher-order harmonic balance methodologies specifically adapted to work efficiently with piecewise-linear nonlinearities.

One of the most ubiquitous nonlinearities usually modeled as piecewise-linear functions is friction, which is most often approximated by

$$\mu N \text{sign}\dot{y}(t) \quad (53)$$

where μ is the coefficient of friction, N is the normal force, $\dot{y}(t)$ is the system's velocity response, and sign is the signum function, equal to 1 if $\dot{y} > 0$, 0 if $\dot{y} = 0$, and -1 if $\dot{y} < 0$. Pierre et al. [5] treated a system containing this nonlinearity using the incremental harmonic balance method around a known solution $\dot{y}_0$. Then a neighboring solution will have a friction force given by

$$\mu N \text{sign}(\dot{y}_0 + \Delta\dot{y}) \quad (54)$$

Expanding this as a Taylor series around u_0 gives

$$\begin{aligned}\mu N\text{sign}(\dot{y}_0 + \Delta\dot{y}) &= \mu N\left(\text{sign}\dot{y}_0 + \Delta\dot{y}\left.\frac{\text{d}[\text{sign}(\dot{y})]}{\text{d}\dot{y}}\right|_{\dot{y}=\dot{y}_0}\right) \\ &= \mu N[\text{sign}\dot{y}_0 + 2\delta(\dot{y}_0)\Delta\dot{y}] \end{aligned} \quad (55)$$

where the derivative of the sign function is taken to be equal to two times the Dirac delta function δ. The rest of the treatment is identical to the IHB method with Galerkin, with sinusoidal basis functions for $\dot{y}_0$ and $\Delta\dot{y}$. The integrals involving $\dot{y}_0$ are calculated numerically, taking care to exactly calculate the zeros of $\dot{y}_0$.

Lau and Zhang [4] performed the calculations outlined earlier on systems with piecewise-linear stiffness. They provided numerical examples for systems with free-play and bilinear stiffnesses (see Fig. 1). As with the friction case, they expanded the nonlinear term in a Taylor series. The Fourier coefficients of the nonlinear function were obtained using the integral definitions of Eqs. (14). The integrations were performed numerically, taking care to calculate the exact moments in time when the system states cross from one piecewise-linear region to another. With reference to Fig. 1, this would mean the exact moments at which the spring displacement is equal to $\pm\delta$. This calculation was performed using a successive bisection numerical scheme. Xu et al. [22] used the same approach on a system containing both stiffness and damping piecewise-linear functions.

K. Quasi-Periodic Limit-Cycle Oscillations

Several authors have tried to treat systems undergoing quasi-periodic LCOs with harmonic balance techniques. Quasi-periodic LCOs are defined as oscillations that never decay, for which the amplitude is approximately constant but which never repeat themselves over any time interval. Figure 2 shows such an oscillation. The signal plotted in the figure never repeats itself but its amplitude never exceeds 0.1 rad. Narrowband chaotic signals are a type of quasi-periodic LCO. It should be stressed that such signals are deterministic.

Lau et al. [18] applied the incremental harmonic balance to a system undergoing quasi-periodic vibrations. They noted that such vibrations have "incommensurable" frequency content. In other words, their frequency content cannot be described by a simple arithmetic progression of the type $(\omega, 2\omega, 3\omega, \ldots, N\omega)$. Instead, the frequencies of quasi-periodic signals can be represented by numerous linear combinations of m different base frequencies,

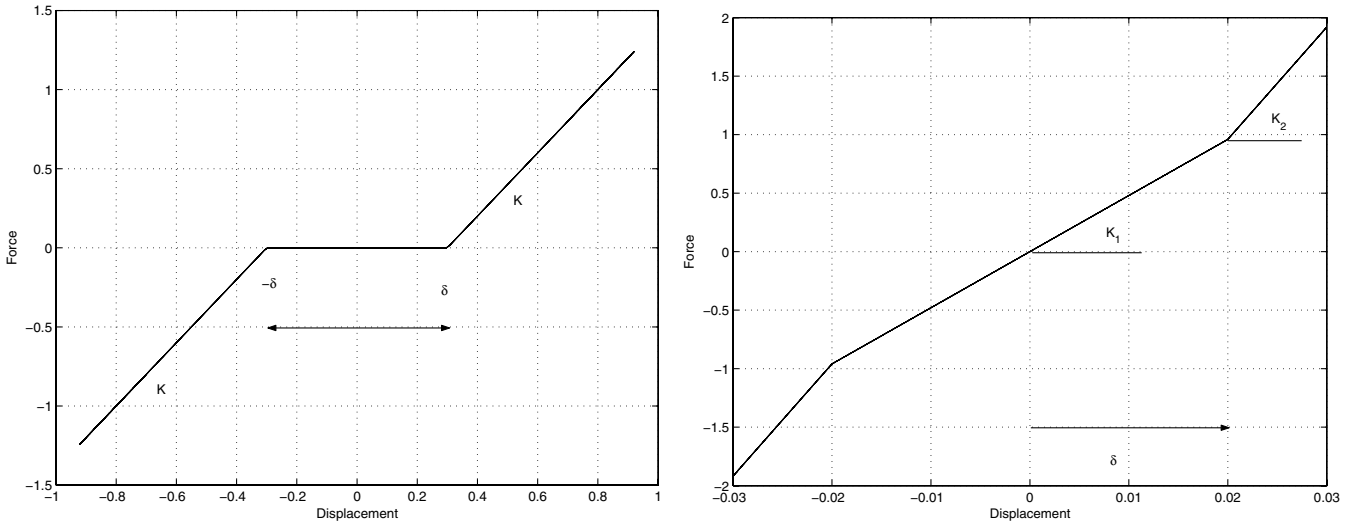

a) Freeplay stiffness **b) Bilinear stiffness**

Fig. 1 Free-play and bilinear stiffness restoring forces.

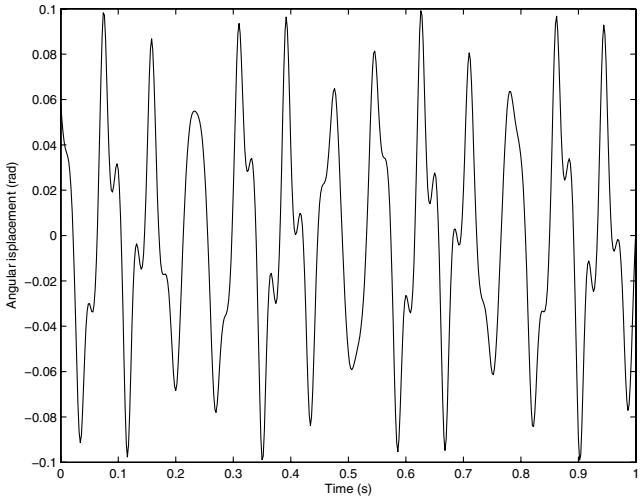

Fig. 2 Example of an quasi-periodic LCO.

$(\omega_1, \omega_2, \omega_2, \ldots, \omega_m)$. Therefore, the sinusoidal expansion Lau et al. used was of the form

$$\mathbf{x} = \sum_{j_1=-N}^{N} \sum_{j_2=-N}^{N} \cdots \sum_{j_m=-N}^{N} \left\{ \mathbf{X}_{j_1,j_2,\ldots,j_m,1} \sin\left(\sum_{k=1}^{m} j_k \omega_k t \right) + \mathbf{X}_{j_1,j_2,\ldots,j_m,2} \cos\left(\sum_{k=1}^{m} j_k \omega_k t \right) \right\} \tag{56}$$

where N is the maximum order of the series. Notice that this expansion is written so that frequencies such as $\omega_1 - 2\omega_2$ are possible. The total number of frequencies is $[(2N+1)^m - 1]/2 + 1$ because some of the linear combinations yield identical sine or cosine waves [e.g., $\cos(3\omega_1 - 3\omega_2)t = \cos(-3\omega_1 + 3\omega_2)t$]. The value of N depends on the degree of nonlinearity of the system, as usual, and the value of m is the number of system states. This type of approach is very computationally expensive because, for example, if only two base frequencies are needed and the maximum order of the harmonic balance is kept to three, then the total number of independent frequencies is 25. For a highly nonlinear system with many states, this procedure becomes prohibitively expensive. Lau et al. [18] applied the approach to a nonlinear vibrating beam but with the limitation that

$$\sum_{k=1}^{m} |j_k| \leq N$$

This reduced the number of acceptable frequency components.

Leung and Fung [25] wrote a paper concerning the "construction of chaotic regions," which is, however, a study of period-doubling behavior, not fully developed chaos. They wrote the sinusoidal expansion for $\mathbf{x}$ as

$$\mathbf{x} = \mathbf{X}_0 + \sum_{k=1}^{\beta N} \left[\mathbf{X}_{k1} \sin\left(\frac{k\omega t}{\beta} \right) + \mathbf{X}_{k2} \cos\left(\frac{k\omega t}{\beta} \right) \right] \tag{57}$$

where β is a positive integer, initially equal to 1. Every time period doubling occurs, β is multiplied by two to reflect the fact that the system's fundamental response frequency is halved. A similar approach was used by Dimitriadis et al. [26] to treat an aeroelastic system exhibiting a secondary Hopf bifurcation. Leung and Fung [25] used Floquet theory to determine when period doubling will occur. Leung and Fung applied this procedure to the Duffing oscillator, whereas Leung and Chui [21] applied it to two coupled Duffing oscillators. It should be noted that, in either case, the system responses for which successful harmonic balance approximations were calculated never exceeded period 6.

l. Time-Domain Harmonic Balance

In this work, the term time-domain harmonic balance (TDHB) is used to describe harmonic balance schemes in which, instead of searching for the correct amplitudes of sine and cosine terms, the search concerns discrete time-domain realizations of the system responses. Such an approach was first developed by Cameron and Griffin [8], which they called the alternating frequency and time (AFT) domain method.

In this approach, the solution of the equations of motion (1) is expressed using its Fourier transform as $\mathbf{X}(\omega)$. The equations of motion are Fourier-transformed to yield

$$\jmath\omega\mathbf{X}(\omega) = \mathbf{F}(\omega) \tag{58}$$

where $\mathbf{F}(\omega)$ is the Fourier transform of $\mathbf{f}(t)$. Instead of the continuous Fourier transform, Cameron and Griffin [8] decided to use the discrete Fourier transform (DFT), evaluated using FFT algorithms. The equations of motion become

$$\jmath k\omega\mathbf{X}_k - \mathbf{F}_k = \mathbf{0} \tag{59}$$

for $k = 0, \ldots, M/2$, where $\mathbf{X}_k$ and $\mathbf{F}_k$ are the values of the kth frequency components of $\mathbf{x}(t)$ and $\mathbf{f}[x(t)]$, respectively. Equations (59) are the DFT equivalent of the harmonic balance governing Eqs. (5). The harmonic balance procedure is modified to search for the values of $\mathbf{X}_k$ that will satisfy Eqs. (59). However, the nonlinear function must, in general, be calculated in the time domain, hence the alternating time- and frequency-domain nature of this method, because the $\mathbf{X}_k$ values must be inverse-Fourier-transformed to obtain time-domain realizations $\mathbf{x}_r$, from which $\mathbf{f}(\mathbf{x}_r)$ is obtained; this is in turn Fourier-transformed to yield the values of $\mathbf{F}_k$ to be substituted into Eq. (59).

With the AFT approach, the order of nonlinearity N is irrelevant. The only consideration is the number of frequency components used. If M is chosen as a power of 2, then FFT procedures can be used. There are, in total, M unknowns in Eqs. (59). These are the real parts $\Re(\mathbf{X}_k)$ for $k = 0, \ldots, M/2$ and the imaginary parts $\Im(\mathbf{X}_k)$ for $k = 1, \ldots, M/2 - 1$. If the frequency ω is also an unknown, then the first element of $\Re(\mathbf{X}_1)$ can be set to be always equal to 0. In cases in which the nonlinear functions in the system are all odd or all even, the AFT procedure can be speeded up by considering only odd or even values of k.

The AFT approach has a disadvantage when used on systems with piecewise-linear nonlinearities. If M is chosen to be low, then the time-domain resolution of $\mathbf{x}_k$ will also be low. However, piecewise-linear functions can only be evaluated accurately if the instances at which the transitions from one piecewise-linear region to another are pinpointed to within a suitable tolerance. One solution to this problem is to always choose the number of samples M to be very high, although this can be an inefficient approach for systems with low orders of nonlinearity. An alternative approach is to create a better sampled time-domain approximation for $\mathbf{x}(t)$, from the FFT coefficients $\mathbf{X}_k$ using a trigonometric interpolation polynomial of the form

$$\mathbf{x}(t) = \mathbf{X}_0 + \sum_{k=1}^{M/2-1} \frac{\mathbf{X}_k}{M} \exp(\jmath\omega k t) + \frac{\mathbf{X}_{M/2}}{M} \cos(\omega M t/2) + \sum_{k=M/2+1}^{M-1} \frac{\mathbf{X}_k}{M} \exp(\jmath\omega(-M+k)t) \tag{60}$$

Equation (60) can be used to calculate $\mathbf{x}(t)$ to any desired resolution and thus obtain highly accurate estimates of $\mathbf{f}[\mathbf{x}(t)]$, even if the nonlinear functions are discontinuous, piecewise-linear, or hysteretic.

Liu et al. [6,7] described a method similar to the AFT, which they call the high-dimensional harmonic balance (HDHB). Instead of using discrete Fourier transforms and inverse Fourier transforms, they use the Fourier series in the form of Eq. (16). Equations (5) are the governing equations of their harmonic balance scheme, and the Fourier series matrices

$$\mathbf{E} = \frac{2}{2N+1} \begin{pmatrix} \frac{1}{2}\mathbf{I} & \frac{1}{2}\mathbf{I} & \cdots & \frac{1}{2}\mathbf{I} \\ \sin k\omega t_0 \mathbf{I} & \sin k\omega t_1 \mathbf{I} & \cdots & \sin k\omega t_{2N} \mathbf{I} \\ \cos k\omega t_0 \mathbf{I} & \cos k\omega t_1 \mathbf{I} & \cdots & \cos k\omega t_{2N} \mathbf{I} \end{pmatrix}$$

and

$$\mathbf{E}^{-1} = \begin{pmatrix} \mathbf{I} & \sin k\omega t_0 \mathbf{I} & \cos k\omega t_0 \\ \vdots & \vdots & \vdots \\ \mathbf{I} & \sin k\omega t_{2N} \mathbf{I} & \cos k\omega t_{2N} \end{pmatrix}$$

are employed to transform from time-domain values to Fourier coefficients and vice versa, where $M = 2N + 1$. The HDHB method suffers from the same problem as the AFT in the presence of discontinuous nonlinearities.

The incremental harmonic balance with discrete Fourier transform used by Leung and Ge [9] can also be included in the TDHB category.

The main advantage of TDHB methods is related to the application to fluid dynamic problems; Hall et al. [27] and Thomas et al. [28,29] applied the HDHB technique to problems involving nonlinear fluid dynamic forces. CFD solvers will typically return values of $\mathbf{x}(t)$ in the time domain. Therefore, it is simpler to perform the harmonic balance iterations in the time domain than in the frequency domain.

III. Continuation Framework

All the harmonic balance methodologies detailed in the previous section are nonlinear problems with iterative solutions. The unknown response amplitudes and frequency (if applicable) are initially guessed and then improved through Newton–Raphson or other types of iteration. Unfortunately, there are no universally applicable rules for choosing the initial guess and, what's more, if the initial guess is too far away from the true solution, the iterative procedure may fail.

In this section, the choice of the initial guess for parameter-dependent systems, such as the system of Eq. (1), will be discussed. The harmonic balance approaches of Sec. II will be placed in a continuation framework in which known solutions at a particular set of parameter values will be continued at new parameter values.

The problem addressed here is similar to the basis of the incremental harmonic balance method in its predictor mode, whereby a solution $\mathbf{x}_0(t)$ at $\mathbf{w}_0$ is continued at $\mathbf{w}_0 + \Delta\mathbf{w}$. However, the IHB approach assumes that $\mathbf{x}_0(t)$ is known, which cannot be the general case. A rigorous solution of Eqs. (1) for all $\mathbf{w}$ values of interest can only be obtained if the character of the response is considered for a very wide range of parameter values, including parameter values for which the system is stable and periodic solutions cannot occur.

A. Stability and Hopf Bifurcation

To render the discussion more coherent, the general form of the system investigated in the following will be simplified to

$$\dot{\mathbf{x}} = \mathbf{f}(\mathbf{x}, t, w) \tag{61}$$

whereby the equations of motion are only dependent on a single parameter: w. It is assumed that the solution to these equations at a particular value of w is not periodic, but constant and equal to $\mathbf{x}_A(w)$, where $\mathbf{x}_A(w)$ is one of the solutions of

$$\dot{\mathbf{x}} = \mathbf{f}(\mathbf{x}, t, w) = \mathbf{0} \tag{62}$$

The stability of the solution can be investigated by linearizing the equations of motion in the neighborhood of $\mathbf{x}_A(w)$. Equations (61) are expanded in a first-order Taylor series as

$$\dot{\mathbf{x}} \approx \left.\frac{\partial \mathbf{f}}{\partial \mathbf{x}}\right|_{\mathbf{x}_A} \mathbf{x} \tag{63}$$

which is valid only when $\mathbf{x}$ is very close to $\mathbf{x}_A$. Equations (63) are a set of first-order linear ordinary differential equations and their solution depends on the eigenvalues of the Jacobian matrix $\partial\mathbf{f}/\partial\mathbf{x}|_{\mathbf{x}_A}$. The solution of Eqs. (63) is assumed to be of the form

$$\mathbf{x} = \mathbf{x}_A + \varepsilon \mathbf{p} \exp \lambda t \tag{64}$$

where ε is a small positive real number, λ is an eigenvalue of the Jacobian, and $\mathbf{p}$ is an eigenvector. Substituting for $\mathbf{x}$ into Eq. (63) and equating orders of ε yields

$$\left(\lambda \mathbf{I} - \left.\frac{\partial \mathbf{f}}{\partial \mathbf{x}}\right|_{\mathbf{x}_A}\right)\mathbf{p} = \mathbf{0} \tag{65}$$

which is an eigenvalue problem to be solved for λ and $\mathbf{p}$. If all the eigenvalues have negative real parts, then $\mathbf{x}_A$ is stable; if one eigenvalue has a positive real part, then the solution is unstable.

Nonlinear algebraic systems of equations may have more than one solution, so that there may well be other possible solutions [say, $\mathbf{x}_B(w), \mathbf{x}_C(w)$, etc.]. At a particular value of w, it can happen that two or more of these solution branches intersect; this intersection is called a bifurcation. A Hopf bifurcation is defined as a bifurcation whereby

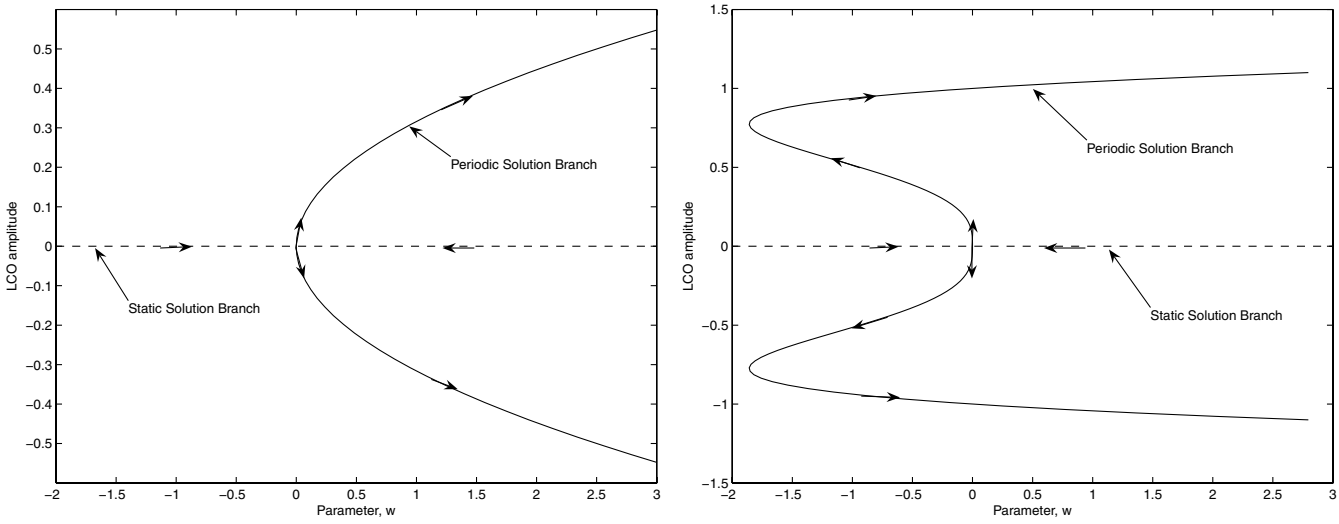

a) Supercritical Hopf **b) Subcritical Hopf**

Fig. 3 Supercritical and subcritical Hopf bifurcations.

a branch of static solutions intersects a branch of periodic solutions. Figure 3 shows two types of Hopf bifurcation: supercritical (whereby LCOs first appear at parameter values higher than the critical parameter value $w = 0$) and subcritical (whereby LCOs first appear at parameter values lower than the critical parameter value). The arrows denote the direction of the continuation process.

For the study of aeroelastic systems undergoing LCOs, the most important type of bifurcation is the Hopf. In general, aeroelastic systems are stable at low values of the airspeed or Mach number; as these parameters are increased, the systems bifurcate to a limit-cycle response. This behavior will be used here to obtain the initial guesses for the harmonic balance methods.

When following a branch of static solutions that intersects a branch of periodic solutions at a value of $w = w_H$, then as this value of the parameter is reached, one pair of eigenvalues λ becomes purely imaginary. The objective is to estimate the value of w_H. This can be done using either an indirect or a direct method [30]. Indirect methods solve for $\Re(\lambda) = 0$ by continuously changing the value of w and calculating the eigenvalues of the Jacobian until a pair of eigenvalues becomes complex. Then they iterate around that neighborhood until w_H is obtained to the desired accuracy. Direct methods set up an augmented system for which the solution converges to the Hopf point (see, for example, [30,31]). Such methods have the advantage of converging monotonously to the Hopf point, but the augmented systems are quite large so that the savings in computational effort can be negligible.

Irrespective of the method employed, when the Hopf point is finally estimated, the values of λ_H and $\mathbf{p}_H$ are also known. At this point, the solution of equation

$$\dot{\mathbf{x}}_H = \mathbf{f}(\mathbf{x}_H, w_h) \tag{66}$$

is known and given by $\mathbf{x}_H = \mathbf{x}_A$. At $w = w_H + \Delta w$, provided Δw is small enough, the first truly periodic solution is assumed to be given by

$$\mathbf{x}_H = \mathbf{x}_A + \varepsilon|\mathbf{p}_H| \sin \omega_H t \tag{67}$$

where ε is an unknown small positive parameter and $|\mathbf{p}_H|$ denotes the magnitude of the elements of $\mathbf{p}_H$. Notice that for a supercritical Hopf bifurcation, Δw must be negative. The assumed solution of Eq. (67) suggests that good initial guesses for a HOHB scheme are

$$\begin{aligned} &\mathbf{X}_0 = \mathbf{x}_A(w_H) \qquad \mathbf{X}_{11} = \varepsilon|\mathbf{p}_H| \qquad \mathbf{X}_{k1} = \mathbf{0} \quad \text{for } k > 1 \\ &\mathbf{X}_{k2} = \mathbf{0} \quad \text{for all } k \qquad \omega = \omega_H \end{aligned} \tag{68}$$

It remains to choose a value for ε. Figure 3 shows that near the Hopf point, the slope of the periodic solutions branch approaches infinity but then decreases. This can be replicated in the harmonic balance scheme by choosing, for example, $\varepsilon = \sqrt{|\Delta w|}$. The initial guesses of Eq. (68) are then fed into the HOHB methodology and the first converged solution is obtained at $w + \Delta w$. The HOHB solution can then be continued along the branch of periodic solutions by increasing the parameter w in small steps and always choosing as the current initial guess the converged solution from the previous value of w. The incremental harmonic balance technique can be continued in its predictor form as long as the previously converged solution lies on the periodic branch.

The starting scheme for HOHB methods discussed earlier is not appropriate for systems with piecewise-linear nonlinearities, such as those shown in Fig. 1. The stability of such systems depends entirely on the stability of the inner linear system (i.e., the system with linear stiffness equal to the stiffness inside the free-play region $[-\delta \quad \delta]$). For a hardening piecewise-linear function, as long as the inner linear system is stable, the nonlinear system admits only static steady-state solutions. When the inner linear system becomes unstable, the nonlinear system admits only periodic solutions. This type of bifurcation is usually termed "explosive" and is graphically visualized in Fig. 4. The initial amplitude of the periodic solution is equal to the width of the free-play region δ.

Piecewise-linear nonlinearities are usually concentrated nonlinear functions of one of the system states or of a single linear combination of the system states. Assume that the nonlinearity only depends on the nth state x_n. Therefore, the simplification for systems with few nonlinear states is adopted. To start a HOHB scheme for a system with piecewise-linear nonlinearity, first the inner linear system must be written as

$$\dot{\mathbf{x}} = \mathbf{Q}_{\text{in}}(w)(\mathbf{x} - \mathbf{x}_A) \tag{69}$$

where $\mathbf{Q}_{\text{in}}(w)$ is a $m \times m$ matrix. The stability of this system depends on the eigenvalues of the $\mathbf{Q}_{\text{in}}$ matrix. Therefore, the value of $w = w_E$ at which a pair of eigenvalues becomes purely imaginary is sought, exactly as in the case of the Hopf bifurcation. When w_E is determined, the oscillation frequency ω_E is also obtained as the imaginary part of the critical eigenvalue. At w_E, the amplitude of vibration of the nonlinear state x_n is equal to δ; that is,

$$x_n = x_{A_n} + \delta \sin \omega_E t \tag{70}$$

At a parameter value of $w_E + \Delta w$, the time history of x_n is assumed to be

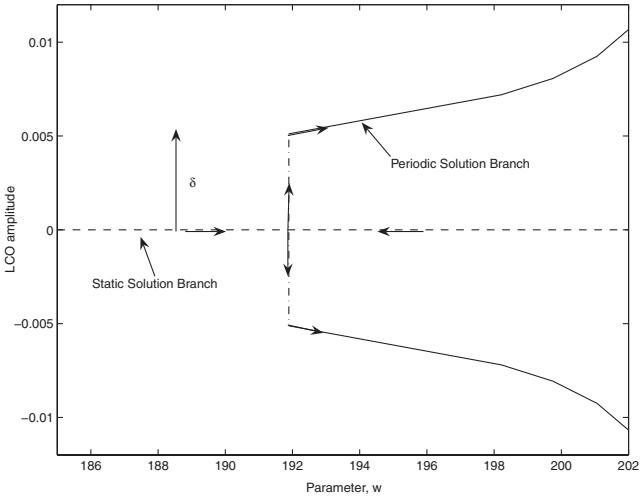

Fig. 4 Explosive bifurcation.

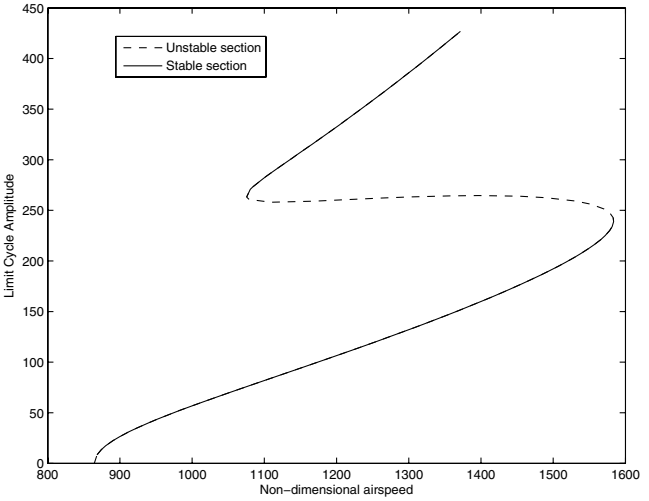

Fig. 5 Fold bifurcation for galloping of a slender prismatic structure.

$$x_n = x_{A_n} + (\delta + \varepsilon)\sin\omega_E t \tag{71}$$

so that the initial guess for a harmonic balance scheme is given by [with respect to Eq. (27)]

$$\begin{aligned} &X_0 = x_{A_n} \qquad X_{11} = \delta + \varepsilon \qquad X_{k1} = 0 \quad \text{for } k > 1 \\ &X_{k2} = 0 \quad \text{for all } k \qquad \omega = \omega_E \end{aligned} \tag{72}$$

Figure 4 shows that the shape of the periodic branch near the bifurcation point is linear, so that $\varepsilon = \Delta w$ is a good choice as long as Δw is small enough.

B. Arc-Length Continuation

In the previous section, a framework was established for initiating a harmonic balance solution at the bifurcation point and continuing it for increasing values of the system parameter. This type of continuation is known as "natural parameter continuation" [32]. It has been noted that the incremental harmonic balance approach is particularly effective at this process in its predictor formulation. In the first applications of the IHB method, the parameter of interest was the frequency of excitation of the system. Pierre et al. [5] and Lau and Zhang [4] both demonstrated the ability of the method to track the system's response amplitude for different values of the frequency of excitation. Kim and Noah [11] used a modified harmonic balance procedure to trace the maximum response amplitude of a system with piecewise-linear stiffness at different values of the excitation frequency. Their technique was not, strictly speaking, a continuation method, because the solutions at each value of the parameter were not related to previous solutions. However, their results showed a weakness of natural parameter continuation in the presence of some types of bifurcation.

Consider the case of a fold bifurcation, such as the one shown in Fig. 5 in which LCO amplitude y is plotted against nondimensional airspeed V. The plot concerns a tall prismatic structure undergoing galloping oscillations [33,34]. At nondimensional airspeed values less than 1075, the system is undergoing low-amplitude limit-cycle oscillations. However, as the airspeed increases, the LCO branch reaches a point ($V = 1584$) at which it folds, moves back toward an airspeed of 1075, and then follows a higher-amplitude path. The solid lines denote stable parts of the LCO branch and the dashed line denotes unstable parts. At airspeeds between 1075 and 1584, there are three visible coexisting limit cycles: two stable and one unstable. A harmonic balance scheme using natural parameter continuation that was started on the low-amplitude LCO will stay on it as the airspeed is increased until, at 1584, it will jump either to the high-amplitude LCO or to the static solution at $y = 0$. Similarly, a scheme started on the high-amplitude LCO will stay on it as the airspeed is decreased until, at 1075, it will jump to the low-amplitude LCO.

An ideal HB continuation scheme should be able to follow the entire LCO branch, despite the fold. The main difficulty is that at the fold, the system Jacobian matrix becomes singular and small changes in parameter values cause large changes in response amplitude. In classical numerical continuation methodologies, bifurcations such as folds are dealt with by means of arc-length and pseudoarc-length continuation (see, for example, Allgower and Georg [35]). In both these approaches, the chosen continuation parameter is not a system parameter but a measure of the distance traveled along the periodic branch.

Leung and Fung [25] first implemented a harmonic balance algorithm that takes advantage of the fact that the Jacobian becomes singular at a fold. The IHB method was modified to look for parameter values at which a fold bifurcation occurs. Values of the parameters for which the Jacobian in the governing IHB equation (46) becomes singular are sought; that is,

$$\det \mathbf{T}_1 = \delta = 0 \tag{73}$$

This relation can be written in incremental form as

$$\left(\frac{\partial\delta}{\partial\mathbf{a}}\right)^T \Delta\mathbf{a} + \left(\frac{\partial\delta}{\partial\mathbf{w}}\right)^T \Delta\mathbf{w} + \delta = 0 \tag{74}$$

Equation (74) is an additional linear equation that can be solved simultaneously with Eqs. (46) to pinpoint folds in the parameter space of the system under investigation. The terms $\partial\delta/\partial\mathbf{a}$ and $\partial\delta/\partial w$ can be calculated either analytically or numerically. It should be noted that this approach is still natural parameter continuation and will not allow the continuation of the solution beyond the fold.

Assuming that there is only one free parameter (say, w), the vector of harmonic balance unknowns can be defined as $\mathbf{a} = [\mathbf{X}_0 \quad \mathbf{X}_{k1} \quad \mathbf{X}_{k2} \quad \omega]^T$. The most logical arc-length parameter s can be defined as the norm of the unknown vector $\mathbf{a}$ and the natural parameter w as

$$s^2 = \mathbf{a}^T\mathbf{a} + w^2 \tag{75}$$

so that the harmonic balance equations (6) become

$$\mathbf{g}[\mathbf{a}(s), w(s)] = \mathbf{0} \tag{76}$$

This procedure is usually called *norm continuation*. It has been shown that norm continuation can fail under certain circumstances (see, for example, Doedel et al. [32]). For this reason, Keller [36] defined a pseudoarc length such that the tangent vector to the periodic solution branch always has unit length; that is,

$$\mathbf{a}'^T\mathbf{a}' + w'^2 = 1 \tag{77}$$

where prime denotes differentiation with respect to s. If the converged HOHB solution at the kth value of the arc-length

parameter s_k is denoted by $\mathbf{a}_k$, then a Taylor expansion of Eq. (77) will yield

$$\mathbf{a}'^{T}_{k-1}\Delta\mathbf{a} + w'_{k-1}\Delta w = \Delta s \tag{78}$$

where prime denotes differentiation with respect to s. Equations (76) and (78) are then solved simultaneously using the following Newton scheme:

$$\begin{pmatrix} \frac{\partial \mathbf{g}}{\partial \mathbf{a}}\Big|_{\mathbf{a}_{i,k},w_{i,k}} & \frac{\partial \mathbf{g}}{\partial w}\Big|_{\mathbf{a}_{i,k},w_{i,k}} \\ \mathbf{a}'^{T}_{k-1} & w'_{k-1} \end{pmatrix} \begin{Bmatrix} \Delta\mathbf{a}_{i,k} \\ \Delta w_{i,k} \end{Bmatrix} = -\begin{Bmatrix} \mathbf{g}(\mathbf{a}_{i,k}, w_{i,k}) \\ (\mathbf{a}_{i,k} - \mathbf{a}_{k-1})^T\mathbf{a}'_{k-1} + (w_{i,k} - w_{k-1})w'_{k-1} - \Delta s \end{Bmatrix} \tag{79}$$

where subscript i denotes the ith iteration, and the $(i+1)$th solution is given by $\mathbf{a}_{i+1,k} = \mathbf{a}_{i,k} + \Delta\mathbf{a}_{i,k}$ and $w_{i+1,k} = w_{i,k} + \Delta w_{i,k}$. The initial solutions at the kth value of the arc-length parameter are obtained from the converged solution at $k-1$ as $\mathbf{a}_{0,k} = \mathbf{a}_{k-1}$ and $w_{0,k} = w_{i-1}$. Once the Newton scheme has converged, the next direction vectors $\mathbf{a}'_k$ and w'_k are calculated from the solution of

$$\begin{pmatrix} \frac{\partial \mathbf{g}}{\partial \mathbf{a}}\Big|_{\mathbf{a}_k,w_k} & \frac{\partial \mathbf{g}}{\partial w}\Big|_{\mathbf{a}_k,w_k} \\ \mathbf{a}'^{T}_{k-1} & w'_{k-1} \end{pmatrix} \begin{Bmatrix} \mathbf{a}'_k \\ w'_k \end{Bmatrix} = \begin{Bmatrix} 0 \\ 1 \end{Bmatrix} \tag{80}$$

Notice that the normalization of the direction vectors achieved with these equations is only approximate, because it depends on previous values of the direction vectors [i.e., Eq. (77) is satisfied only approximately]. Perfect normalization can be achieved by dividing the direction vectors resulting from Eq. (80) by their norm; that is,

$$\sqrt{\mathbf{a}'^{T}_k\mathbf{a}'_k + w'^{2}_k}$$

The solutions for $k = 0, 1$ are obtained from the Hopf or explosive bifurcation analysis described earlier. The case $k = 0$ corresponds to the exact bifurcation parameter value, and the case $k = 1$ corresponds to the bifurcation parameter increased by Δw. For these two cases, the arc-length parameter can be calculated using Eq. (75) so that the first direction vectors are obtained as

$$\mathbf{a}'_1 = (\mathbf{a}_1 - \mathbf{a}_0)/(s_1 - s_0) \qquad w'_1 = (w_1 - w_0)/(s_1 - s_0)$$

with subsequent normalization by the norm of the tangent vector. For $k > 1$, the pseudoarc-length equations (79) and (80) are used.

Leung and Chui [21] implemented a pseudoarc-length scheme by defining the pseudoarc-length parameter as

$$s_k = \{(\mathbf{q}_{k-1} - \mathbf{q}_{k-2})/\|\mathbf{q}_{k-1} - \mathbf{q}_{k-2}\|\}^T(\mathbf{q}_k - \mathbf{q}_{k-1}) \tag{81}$$

where $\mathbf{q} = [\,\mathbf{a}^T \quad w\,]^T$ for $k > 2$. Therefore, s is defined in terms of two previous points on the LCO branch. Equations (46) are extended to

$$\begin{pmatrix} \mathbf{T}_1 & \mathbf{T}_2 \\ (\mathbf{a}_{k-1} - \mathbf{a}_{k-2})/\|\mathbf{q}_{k-1} - \mathbf{q}_{k-2}\| & (w_{k-1} - w_{k-2})/\|\mathbf{q}_{k-1} - \mathbf{q}_{k-2}\| \end{pmatrix} \times \begin{Bmatrix} \Delta\mathbf{a} \\ \Delta w \end{Bmatrix} = \begin{Bmatrix} \mathbf{R}_0 \\ \Delta s \end{Bmatrix} \tag{82}$$

Von Groll and Ewins [14] used the arc-length definition of Eq. (77) but chose a different discretization procedure by writing [37]

$$(\mathbf{q}_i - \mathbf{q}_{i-1})^T(\mathbf{q}_i - \mathbf{q}_{i-1}) - \Delta s^2 = 0 \tag{83}$$

The advantage of this equation over the Leung and Chui [21] expression (81) is that only one previous value of $\mathbf{q}$ is required to perform the continuation. Von Groll and Ewins [14] implemented this scheme on the harmonic balance method with Newton–Raphson.

It should be noted that several researchers have used arc-length continuation with HOHB methods on different applications. Von Groll and Ewins [14] applied higher-order harmonic balance with Newton–Raphson and arc-length continuation to rotor/stator contact problems. Raghothama and Narayan [38] applied the methodology of Leung and Chui [21] to a geared rotor-bearing system and a pitch-plunge airfoil with cubic stiffness [39]. However, all of these efforts addressed only systems undergoing supercritical Hopf bifurcations.

The pseudoarc-length harmonic balance scheme described here can be applied in an identical manner to time-domain harmonic balance approaches.

IV. Application to Aircraft Example

The aeroelastic example used in this work is a GTA modeled using finite elements and doublet-lattice unsteady aerodynamics. The modeling was performed by means of the MSC.Nastran software. The same model was used by this author in a study of numerical continuation methods for nonlinear aeroelastic systems [40]. The aerodynamic and structural grids for the GTA are shown in Fig. 6. The aircraft features an unswept rectangular wing and a T-tail. No engines are modeled. The finite element grid contains 678 degrees of freedom and is composed of bar elements. Five control surfaces are modeled: two ailerons, two elevators, and a rudder. The equations of motion were written in modal space, retaining the first seven modes calculated from the MSC.Nastran solution. The aerodynamic influence coefficient matrix for these modes was calculated as a function of frequency and then expanded as a rational fraction polynomial with four aerodynamic lags using Roger's approximation [41] to transform the equations of motion to the time domain.

The final equations of motion are written in first-order form as

$$\dot{\mathbf{x}} = \mathbf{Q}\mathbf{x} \tag{84}$$

where $\mathbf{x}$ is a state vector with $m = 42$ elements, 7 modal velocities $\dot{\mathbf{u}}$, 7 modal displacements $\mathbf{u}$, and 4×7 aerodynamic states $\mathbf{v}$, so that $\mathbf{x} = [\,\dot{\mathbf{u}}^T \quad \mathbf{u}^T \quad \mathbf{v}^T\,]^T$. The matrix $\mathbf{Q}$ is a 42×42 matrix that depends on the airspeed V and air density ρ. Therefore, the parameter vector in the general equation of motion (1) becomes $\mathbf{w} = [\,V \quad \rho\,]^T$.

The equation of motion (84) is completely linear. Nonlinearities can be added in the rotations of any of the control surfaces. In the present case, stiffness nonlinearity was added to the aileron rotation. The introduction of nonlinearity could be performed in modal space because large changes in the aileron stiffness did not significantly affect the system's mode shapes. The corresponding elements of the structural stiffness matrix in physical space were set to zero and the matrix was then transformed to the modal domain; finally, the nonlinear term was added. The equations of motion become

$$\dot{\mathbf{x}} = \bar{\mathbf{Q}}\mathbf{x} + \mathbf{q}f(\mathbf{x}) \tag{85}$$

where $\bar{\mathbf{Q}}$ is the modified state matrix, f is a nonlinear function, and $\mathbf{q}$ is a $m \times 1$ vector transforming the nonlinearity from physical space to modal space. The finite element grid defines the aileron rotation as the difference between the rotations of two grid-points (say, r_1 and r_2). Therefore, the nonlinearity is a function of two coordinates in physical space but all of the coordinates in modal space. Denote the control rotation by y so that

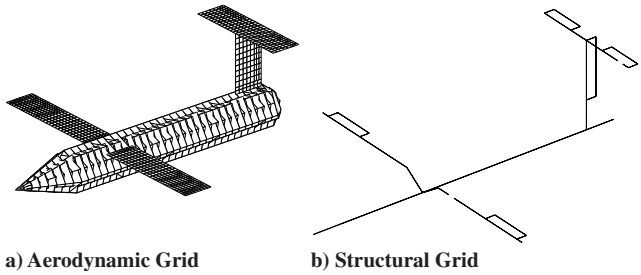

a) Aerodynamic Grid b) Structural Grid

Fig. 6 Aerodynamic and structural grids for GTA model [40].

$$y = (\mathbf{\Phi}_{r_1} - \mathbf{\Phi}_{r_2})\mathbf{u} \tag{86}$$

where $\mathbf{\Phi}$ is the 678×7 modal transformation matrix, transforming from modal to physical coordinates, and the subscripts r_1 and r_2 denote the r_1th and r_2th rows of $\mathbf{\Phi}$, respectively. Therefore, the nonlinear function depends on a linear combination of all the modal displacements. Equation (86) can equally be written as

$$y = \mathbf{c}\mathbf{x} \tag{87}$$

where $\mathbf{c}$ is a 1×42 vector given by $\mathbf{c} = [0 \quad \cdots \quad 0 \quad (\mathbf{\Phi}_{r_1} - \mathbf{\Phi}_{r_2}) \quad 0 \quad \cdots \quad 0]$. The harmonic balance method is applied to the system by expressing y as

$$y(t) = Y_0 + \sum_{k=1}^{N} (Y_{k1} \sin k\omega t + Y_{k2} \cos k\omega t) \tag{88}$$

The nonlinear functions chosen for this work are polynomial and free-play stiffness. Polynomial stiffness was chosen to demonstrate the performance of harmonic balance methods on a system undergoing a subcritical Hopf and numerous fold bifurcations. Free play was chosen to apply HB to a system with an explosive bifurcation. The polynomial stiffness function is given by

$$f(y) = K_1 y + K_2 y|y| + K_3 y^3 \tag{89}$$

where K_1, K_2, and K_3 are the linear, quadratic, and cubic stiffness coefficients, respectively. When the quadratic stiffness coefficient is less than zero, the nonlinearity can cause the system to undergo a subcritical Hopf bifurcation. The free-play stiffness (see Fig. 1a) is equal to

$$f(y) = \begin{cases} K(y - \delta) & \text{if } y \geq \delta \\ 0 & \text{if } \delta < y < \delta \\ K(y + \delta) & \text{if } y \leq \delta \end{cases} \tag{90}$$

Because the equations of motion (85) for the GTA are of the form of Eqs. (26), the simplification for systems with few nonlinear states can be employed.

Arc-length continuation schemes work best when ω and w and $[\mathbf{X}_0^T \quad \mathbf{X}_{k1}^T \quad \mathbf{X}_{k2}^T]^T$ and $[\mathbf{X}_0^T \quad \mathbf{X}_{k1}^T \quad \mathbf{X}_{k2}^T]$ are of the same order. In the case of aeroelastic systems, the vibration responses are usually less than one, whether they represent displacements measured in meters or feet or rotations measured in radians. The radial frequency ω is generally $\mathcal{O}(10)$ or $\mathcal{O}(10^2)$, the density in kilograms per cubic meter is $\mathcal{O}(1)$ or $\mathcal{O}(10^{-1})$, and the airspeed $\mathcal{O}(10^2)$ is measured in knots or meters per second. Therefore, the parameters must be normalized so that they are of the same order as the vibration response amplitudes. In this work, the normalization was performed by writing the harmonic balance in terms of period (measured in seconds) instead of radial frequency and by measuring the airspeed in kilometers per second. The density was not used as an active parameter and therefore was not normalized.

All the harmonic balance results presented for the GTA are compared with numerical integration (time marching) solutions obtained using a fifth-order Runge–Kutta method [42]. For the polynomial stiffness case, K_1 was chosen as equal to zero; $K_2 = -K_l/100$, where K_l is the linear stiffness of the control surface; and $K_3 = 10^4 K_l$. For the free-play case, $K = K_l$ and $\delta = 0.005$ rad.

A. Harmonic Balance with Newton–Raphson and Incremental Harmonic Balance

As already argued in this work, although the harmonic balance and incremental harmonic balance are conceptually different, the results obtained from the methods are identical. Therefore, only results from the harmonic balance method will be presented.

Figure 7 shows the limit-cycle amplitudes predicted by the harmonic balance with Newton–Raphson method for the GTA model with polynomial stiffness. Four sets of results are shown, obtained from HB with orders 1, 3, and 11 and from numerical integration. It should be noted that all the HB calculations take advantage of the fact that the nonlinearity is odd and make use only of odd orders.

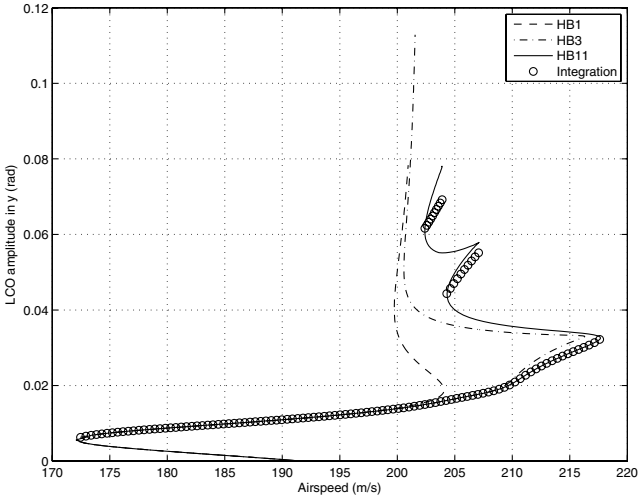

Fig. 7 LCO amplitudes predicted by harmonic balance with Newton–Raphson for polynomial stiffness case.

The results obtained from the numerical integration show that the system begins to undergo LCOs at 172 m/s and the first oscillations start to occur at a nonzero amplitude. The LCO amplitude increases steadily with airspeed up to an airspeed of 217 m/s, when unbounded diverging oscillations start to occur. Additionally, between 202 and 207 m/s, two more limit cycles are possible at higher amplitudes.

The harmonic balance results identify the airspeed of 192 m/s as the bifurcation airspeed. This also happens to be the linear flutter speed. An unstable LCO begins to grow from zero amplitude at the bifurcation point as the airspeed decreases. When the airspeed reaches 172 m/s, the direction of the LCO branch changes and moves toward positive airspeeds, whereas the LCO itself becomes stable. This phenomenon is characteristic of subcritical Hopf bifurcations, as shown in Fig. 3b. The first-order harmonic balance predicts a branch for which the amplitude increases steadily until 200 m/s, when it shoots off to high values. The third-order harmonic balance results follow the LCO branch up to 216 m/s and then fold over toward 200 m/s, at which point they also shoot off. Finally, the 11th-order HB solution correctly follows the LCO branch through five folds and predicts amplitudes very close to those obtained from numerical integration. Liu and Dowell [43] also noted that significantly higher-harmonic-balance orders are needed to accurately predict secondary bifurcations (folds, in the present case).

Figure 8 shows the limit-cycle frequencies predicted by the harmonic balance with Newton–Raphson method for the GTA model with polynomial stiffness. It can be seen that the higher-amplitude parts of the LCO branch also have higher frequency. The first-order HB results only predict the first fold and miss the subsequent folds. The third-order HB scheme predicts three folds in total, whereas the 11th-order scheme correctly predicts all the folds and yields frequencies very close to those calculated from the numerical integration procedure.

Figure 9 shows the limit-cycle amplitudes predicted by the harmonic balance with Newton–Raphson method for the GTA model with free-play stiffness. Again, results for HB orders of 1, 3, and 11 are shown, together with the numerical integration results. This bifurcation diagram is much simpler than the one obtained for the polynomial stiffness. There are no folds and at each airspeed only one limit cycle is possible. The simplicity of the bifurcation behavior increases the accuracy of all HB schemes. Even the first-order scheme yields a highly accurate LCO branch. The 3rd- and 11th-order results are virtually identical to those obtained from numerical integration.

It should be stressed that in this case, the continuation scheme has worked despite the fact that the bifurcation encountered is not a Hopf. Because the LCO amplitude jumps from 0 to δ at the bifurcation

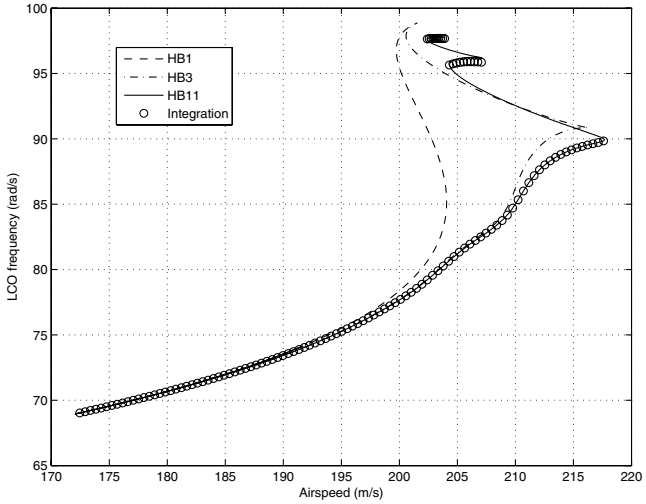

Fig. 8 LCO frequencies predicted by harmonic balance with Newton–Raphson for polynomial stiffness case.

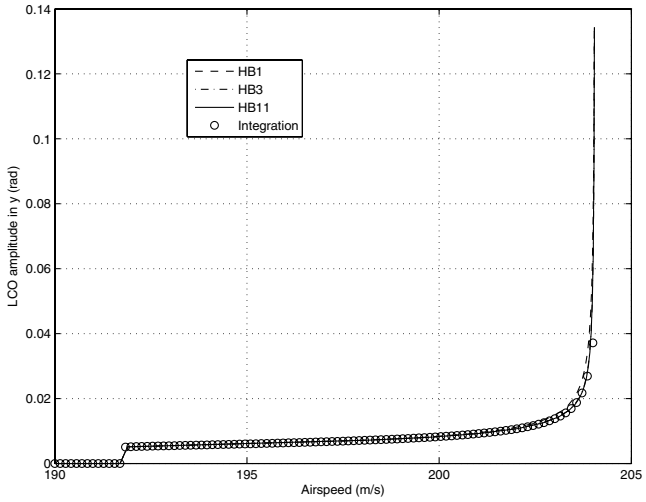

Fig. 9 LCO amplitudes predicted by harmonic balance with Newton–Raphson for free-play stiffness case.

point, the choice of initial solution for all harmonic balance schemes is very straightforward.

The same degree of accuracy can be seen in the LCO frequency results for the GTA model with free-play stiffness, as shown in Fig. 10.

B. Alternating Frequency- and Time-Domain Method and High-Density Harmonic Balance

Figure 11 plots the LCO amplitudes calculated for the GTA model with polynomial stiffness from AFT procedures of $M = 8$ to 32. It can be seen that all solutions can follow the LCO branch accurately from the bifurcation point to an airspeed of 205 m/s. At that point, the eighth-order solution diverges from the LCO branch and follows a rather fancy path. The 16th-order solution follows the LCO branch up to 217 m/s and goes through the first fold but then leaves the branch and eventually moves in the decreasing airspeed direction. Finally, the order-32 solution is highly accurate and follows all the folds.

The AFT method is more computationally expensive than the standard harmonic balance. The example of Fig. 11 shows that similar results are obtained from an order-32 AFT scheme as from an order-11 HB scheme. Despite the speed of FFT algorithms, calculating Jacobians of size 32×32 is twice as expensive as the calculation of the 23×23 Jacobians required for the HB method. By taking advantage of the fact that the nonlinear function is odd, the

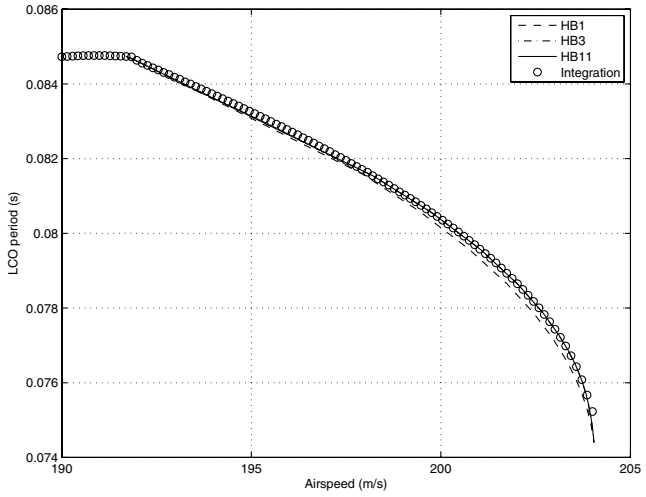

Fig. 10 LCO frequencies predicted by harmonic balance with Newton–Raphson for free-play stiffness case.

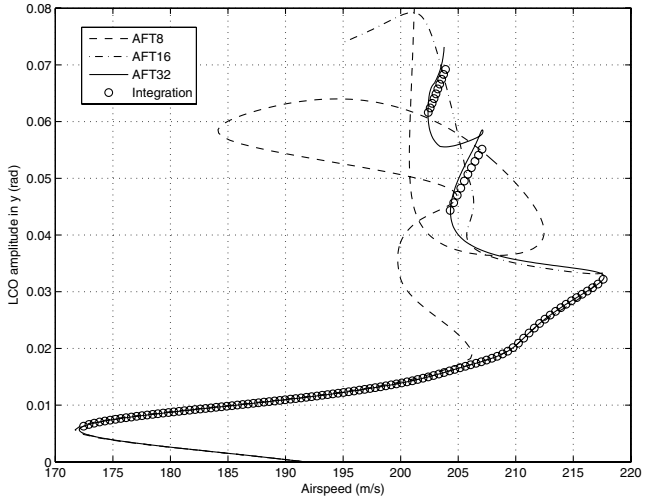

Fig. 11 LCO amplitudes predicted by Alternating Frequency time-domain method for polynomial stiffness case.

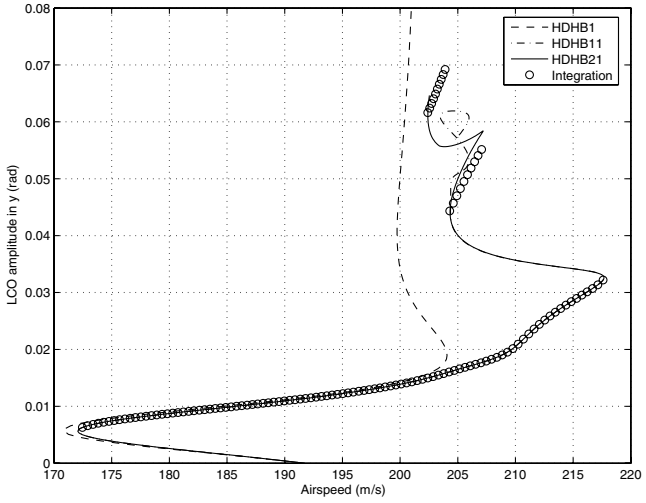

Fig. 12 LCO amplitudes predicted by high-density harmonic balance method for polynomial stiffness case.

size of the AFT Jacobian decreases to 17×17, whereas that of the HB Jacobian shrinks to 13×13. The AFT method is still 70% more expensive than the HB approach.

The high-density harmonic balance method is more successful than the AFT approach at low orders but is still more computationally expensive than the standard harmonic balance technique. Figure 12 plots three LCO amplitude results calculated for the GTA model with polynomial stiffness from HDHB procedures, from solutions of orders 1, 11, and 21. It can be seen that the first-order solution features some inaccuracy in the neighborhood of the first fold. It then follows the actual LCO branch closely up to an airspeed of 205 m/s. The 11th-order solution is quite accurate up to the third fold but then fails. Finally, the 21st-order solution is accurate throughout the LCO branch. The HDHB yields the same degree of accuracy as the standard harmonic balance method but at higher orders and, hence, computational cost.

The main difference between the standard harmonic balance and the time-domain harmonic balance methods is the fact that for the latter, the Jacobian is set up by calculating the rate of change of the harmonic balance equations to changes in time-domain values of the responses, as opposed to Fourier series coefficients. Because the Jacobians are calculated numerically, dependence on time-domain values can cause inaccuracies. Consider the case in which the Jacobian is calculated for the GTA aircraft with nonlinearity in the control surface stiffness using Eq. (22). For the harmonic balance method, the Jacobian is given by

$$\frac{1}{\delta y}\left([\mathbf{g}(Y_0 + \delta y) - \mathbf{g}(Y_0)] \quad [\mathbf{g}(Y_{11} + \delta y) - \mathbf{g}(Y_{11})] \quad \ldots \quad [\mathbf{g}(Y_{N2} + \delta y) - \mathbf{g}(Y_{N2})] \right)$$

where $\mathbf{g} = [\,(Y_0 - \hat{Y}_{0_n})^T \quad (Y_{k1} - \hat{Y}_{k1_n})^T \quad (Y_{k2} - \hat{Y}_{k2_n})^T\,]^T$, following the simplification for systems with few nonlinear states [Eq. (34)], and the notation $\mathbf{g}(Y_0 + \delta y)$ is shorthand for $\mathbf{g}(Y_0 + \delta y, Y_{11}, \ldots, Y_{N2})$. Increasing the Y_0 or Y_{11} coefficient by a small amount δy results in a new Fourier series. For TDHB approaches, the Jacobian is given by

$$\frac{1}{\delta y}\left([\mathbf{g}(y_0 + \delta y) - \mathbf{g}(y_0)] \quad [\mathbf{g}(y_2 + \delta y) - \mathbf{g}(y_2)] \quad \ldots \quad [\mathbf{g}(y_{2N}) + \delta y) - \mathbf{g}(y_{2N})] \right)$$

Although the original time signal y_k was an exact Fourier series, increasing one of the y_k values by a small amount results in a new signal that is not an exact Fourier series. The modified signal can only be accurately rendered as a Fourier series if the order of the series is high, hence the reduced accuracy of THDB methods at low orders.

It should be mentioned that from a practical engineering point of view, the airspeed at which multiple LCOs start appearing (i.e., around 202 m/s) is the maximum safe airspeed. Up to that point, the LCO amplitude is predictable and any combination of initial conditions and/or external excitation will lead the system to either a stable solution (only possible at airspeeds less than 192 m/s) or the single possible limit cycle. At airspeeds greater than 202 m/s, the LCO amplitude depends strongly on the initial conditions. For the purposes of the present work, the LCO branch was continued only through the first five folds. However, there are many more folds in the same airspeed range, leading to possible LCOs of even higher amplitudes. In practical terms, 202 m/s is the flutter speed. All HB schemes presented here, even the first-order schemes, will follow the LCO branch with reasonable accuracy up to that airspeed. As such, although higher-order HB schemes can follow the LCO branch for longer and with greater accuracy, they are of limited practical use.

The results obtained from both TDHB methods for the GTA model with free-play stiffness are very similar to those obtained from the HB method (as shown in Figs. 9 and 10) and therefore are not presented in this work.

V. Conclusions

This paper presented a thorough discussion of the harmonic balance method and several of its variants. The methods were integrated into a continuation framework to enable them to follow the complete dynamic behavior of a nonlinear system undergoing limit-cycle oscillations from the bifurcation point to any desired value of the controlling parameter. It is shown that this framework can be started at subcritical and supercritical Hopf bifurcations and can successfully negotiate fold bifurcations.

The harmonic balance methods were applied to a nonlinear aeroelastic model of a transport aircraft with nonlinear stiffness in the control surface. It was demonstrated that high-order solutions can calculate the complete bifurcation behavior, following the LCO branch with very good accuracy, starting at a subcritical Hopf or explosive bifurcation, and continuing through a number of successive fold bifurcations.

On the other hand, low-order HB solutions managed to capture the essence of the bifurcation behavior of the system even when they could not closely follow a branch through the numerous fold bifurcations. Such solutions predicted LCO amplitudes tending to infinity at points at which the true LCO branch is going through folds, resulting in several possible LCOs of increasing amplitude at the same airspeed. Nevertheless, the results obtained were practically significant because they were valid up to the maximum safe flight airspeed. Furthermore, they were obtained at significantly lower computational cost.

Finally, it was found that time-domain harmonic balance approaches are more computationally expensive than the standard harmonic balance methods. The former can produce LCO branch predictions as accurate as those obtained from the latter, but only if higher orders of approximation are used.

References

[1] Kryloff, N., and Bogoliuboff, N., *Introduction to Nonlinear Mechanics*, Princeton Univ. Press, Princeton, NJ, 1947.

[2] Ling, F. H., and Wu, X. X., "Fast Galerkin Method and Its Application to Determine Periodic Solutions of Nonlinear Oscillators," *International Journal of Non-Linear Mechanics*, Vol. 22, No. 2, 1987, pp. 89–98. doi:10.1016/0020-7462(87)90012-6

[3] Ferri, A. A., and Dowell, E. H., "Frequency Domain Solutions to Multi-Degree-of-Freedom, Dry Friction Damped Systems," *Journal of Sound and Vibration*, Vol. 124, No. 2, 1988, pp. 207–224. doi:10.1016/S0022-460X(88)80183-4

[4] Lau, S. L., and Zhang, W. S., "Nonlinear Vibrations of Piecewise-Linear Systems by Incremental Harmonic Balance Method," *Journal of Applied Mechanics*, Vol. 59, No. 1, 1992, pp. 153–160.

[5] Pierre, C., Feri, A. A., and Dowell, E. H., "Multi-Harmonic Analysis of Dry Friction Damped Systems Using and Incremental Harmonic Balance Method," *Journal of Applied Mechanics*, Vol. 52, No. 4, 1985, pp. 958–964.

[6] Liu, L., "Higher Order Harmonic Balance Analysis for Limit Cycle Oscillations in an Airfoil with Cubic Restoring Forces," 46th AIAA/ASME/ASCE/AHS/ASC Structures, Structural Dynamics & Materials Conference, Austin, TX, AIAA Paper 2005-1918, Apr. 2005.
[7] Liu, L., and Dowell, E. H., "Harmonic Balance Approach for an Airfoil with a Freeplay Control Surface," *AIAA Journal*, Vol. 43, No. 4, 2005, pp. 802–815.
[8] Cameron, T. M., and Griffin, J. H., "An Alternating Frequency/Time Domain Method for Calculating the Steady-State Response of Nonlinear Dynamic Systems," *Journal of Applied Mechanics*, Vol. 56, No. 1, 1989, pp. 149–153.
[9] Leung, A. Y. T., and Ge, T., "Toeplitz Jacobian Matrix for Nonlinear Periodic Vibration," *Journal of Applied Mechanics*, Vol. 62, No. 3, 1995, pp. 709–717.
[10] Ge, T., and Leung, A. Y. T., "A Toeplitz Jacobian Matrix/Fast Fourier Transform Method for Steady-State Analysis of Discontinuous Oscillators," *Shock and Vibration*, Vol. 2, No. 3, 1995, pp. 205–218.
[11] Kim, Y. B., and Noah, S. T., "Stability and Bifurcation Analysis of Oscillators with Piecewise Linear Characteristics: A General Approach," *Journal of Applied Mechanics*, Vol. 58, No. 2, 1991, pp. 545–553.
[12] Tamura, H., Tsuda, Y., and Sueoka, A., "Higher Approximation of Steady Oscillations in Nonlinear Systems with Single Degree Of Freedom," *Bulletin of the JSME*, Vol. 23, No. 195, 1981, pp. 1616–1624.
[13] Broyden, C. G., "A Class of Methods for Solving Nonlinear Simultaneous Equations," *Mathematics of Computation*, Vol. 19, No. 92, 1965, pp. 577–593. doi:10.2307/2003941
[14] Von Groll, G., and Ewins, D. J., "The Harmonic Balance Method with Arc-Length Continuation in Rotor/Stator Contact Problems," *Journal of Sound and Vibration*, Vol. 241, No. 2, 2001, pp. 223–233. doi:10.1006/jsvi.2000.3298
[15] Popov, E. P., "On the Use of the Harmonic Linearization Method in Automatic Control Theory," NACA, TM 1406, 1957.
[16] Lee, B. H. K., Liu, L., and Chung, K. W., "Airfoil Motion in Subsonic Flow with Strong Cubic Restoring Forces," *Journal of Sound and Vibration*, Vol. 281, Nos. 3–5, 2005, pp. 699–717. doi:10.1016/j.jsv.2004.01.034
[17] Lau, S. L., Cheung, Y. K., and Wu, S. Y., "A Variable Parameter Incrementation Method for Dynamic Instability of Linear and Nonlinear Systems," *Journal of Applied Mechanics*, Vol. 49, No. 4, 1982, pp. 849–853.
[18] Lau, S. L., Cheung, Y. K., and Wu, S. Y., "Incremental Harmonic Balance Method with Multiple Time Scales for Aperiodic Vibration of Nonlinear Systems," *Journal of Applied Mechanics*, Vol. 50, No. 4A, 1983, pp. 871–876.
[19] Ferri, A. A., "On the Equivalence of the Incremental Harmonic Balance Method and the Harmonic Balance-Newton–Raphson Method," *Journal of Applied Mechanics*, Vol. 53, June 1986, pp. 455–457.
[20] Lau, S. L., and Yuen, S. W., "Solution Diagram of Nonlinear Dynamic Systems with the IHB Method," *Journal of Sound and Vibration*, Vol. 167, No. 2, 1993, pp. 303–316. doi:10.1006/jsvi.1993.1337
[21] Leung, A. Y. T., and Chui, S. K., "Non-Linear Vibration of Coupled Duffing Oscillators by an Improved Incremental Harmonic Balance Method," *Journal of Sound and Vibration*, Vol. 181, No. 4, 1995, pp. 619–633. doi:10.1006/jsvi.1995.0162
[22] Xu, L., Lu, M. W., and Cao, Q., "Bifurcation and Chaos of a Harmonically Excited Oscillator with Both Stiffness and Viscous Damping Piecewise Linearities by Incremental Harmonic Balance Methods," *Journal of Sound and Vibration*, Vol. 264, No. 4, 2003, pp. 873–882. doi:10.1016/S0022-460X(02)01194-X
[23] Chung, K. W., Chan, C. L., and Xu, J., "An Efficient Method for Switching Branches of Period-Doubling Bifurcations of Strongly Nonlinear Autonomous Oscillators with Many Degrees of Freedom," *Journal of Sound and Vibration*, Vol. 267, No. 4, 2003, pp. 787–808. doi:10.1016/S0022-460X(02)01437-2
[24] Yang, Z. C., and Zhao, L. C., "Analysis of Limit Cycle Flutter of an Airfoil in Incompressible Flow," *Journal of Sound and Vibration*, Vol. 123, No. 1, 1988, pp. 1–13. doi:10.1016/S0022-460X(88)80073-7
[25] Leung, A. Y. T., and Fung, T. C., "Construction of Chaotic Regions," *Journal of Sound and Vibration*, Vol. 131, No. 3, 1989, pp. 445–455. doi:10.1016/0022-460X(89)91004-3
[26] Dimitriadis, G., Vio, G., and Cooper, J. E., "Application of Higher-Order Harmonic Balance to Non-Linear Aeroelastic Systems," 47th AIAA/ASME/ASCE/AHS/ASC Structures, Structural Dynamics and Materials Conference, Newport, RI, AIAA Paper 2006-2023, May 2006.
[27] Hall, K. C., Thomas, J. P., and Clark, W. S., "Computation of Unsteady Nonlinear Flows in Cascades Using a Harmonic Balance Technique," *AIAA Journal*, Vol. 40, No. 5, 2002, pp. 879–886.
[28] Thomas, J. P., Dowell, E. H., and Hall, K. C., "Nonlinear Inviscid Aerodynamic Effects on Transonic Divergence, Flutter and Limit-Cycle Oscillations," *AIAA Journal*, Vol. 40, No. 4, 2002, pp. 638–646.
[29] Thomas, J. P., Dowell, E. H., and Hall, K. C., "Modeling Viscous Transonic Limit-Cycle Oscillation Behavior Using a Harmonic Balance Approach," *Journal of Aircraft*, Vol. 41, No. 6, 2004, pp. 1266–1274.
[30] Griewank, A., and Reddien, G., "The Calculation of Hopf Points by a Direct Method," *IMA Journal of Numerical Analysis*, Vol. 3, No. 3, 1983, pp. 295–303. doi:10.1093/imanum/3.3.295
[31] Roose, D., and Hlavaček, V., "A Direct Method for the Computation of Hopf Points," *SIAM Journal on Applied Mathematics*, Vol. 45, No. 6, 1985, pp. 879–894. doi:10.1137/0145053
[32] Doedel, E., Keller, H. B., and Kernevez, J. P., "Numerical Analysis and Control of Bifurcation Problems, 1: Bifurcation in Finite Dimensions," *International Journal of Bifurcation and Chaos in Applied Sciences and Engineering*, Vol. 1, No. 3, 1991, pp. 493–520. doi:10.1142/S0218127491000397
[33] Vio, G., Dimitriadis, G., and Cooper, J., "On the Solution of the Aeroelastic Galloping Problem," *International Conference on Noise and Vibration Engineering (ISMA2004)*, Katholieke Univ Leuven, Dept. of Mechanical Engineering, Leuven, Belgium, Sept. 2004, Paper 247.
[34] Vio, G. A., Dimitriadis, G., and Cooper, J. E., "Bifurcation Analysis and Limit Cycle Oscillation Amplitude Prediction Methods Applied to the Aeroelastic Galloping Problem," *Journal of Fluids and Structures* (to be published).
[35] Allgower, E. L., and Georg, K., *Numerical Continuation Methods: An Introduction*, Springer–Verlag, New York, 1990.
[36] Keller, H. B., "Numerical Solution of Bifurcations and Nonlinear Eigenvalue Problems," *Applications of Bifurcation Theory*, edited by P. H. Rabinowitz, Academic Press, New York, 1977, pp. 359–384.
[37] Nayfeh, A., and Balachandran, B. (eds.), *Applied Nonlinear Dynamics*, Wiley, New York, 1995.
[38] Raghothama, A., and Narayanan, S., "Bifurcation and Chaos in Geared Rotor Bearing System by Incremental Harmonic Balance," *Journal of Sound and Vibration*, Vol. 226, No. 3, 1999, pp. 469–492. doi:10.1006/jsvi.1999.2264
[39] Raghothama, A., and Narayanan, S., "Non-Linear Dyamics of a Two-Dimensional Airfoil by Incremental Harmonic Balance Method," *Journal of Sound and Vibration*, Vol. 226, No. 3, 1999, pp. 493–517. doi:10.1006/jsvi.1999.2260
[40] Dimitriadis, G., "Bifurcation Analysis for Subsonic Nonlinear Aircraft Using Numerical Continuation," *Journal of Aircraft* (submitted for publication).
[41] Roger, K. L., "Airplane Math Modelling Methods for Active Control Design," AGARD, Rept. AGARD-CP-228, 1977.
[42] Gerald, C. F., and Wheatley, P. O., *Applied Numerical Analysis*, 5th ed., Addison–Wesley, Reading, MA, 1990.
[43] Liu, L., and Dowell, E. H., "The Secondary Bifurcation of an Aeroelastic Airfoil Motion: Effect of Higher Harmonics," *Nonlinear Dynamics*, Vol. 37, No. 1, 2004, pp. 31–49. doi:10.1023/B:NODY.0000040033.85421.4d